IEEE Access
Multidisciplinary | Rapid Review | Open Access Journal

Received 2 April 2026, accepted 21 May 2026, date of publication 25 May 2026, date of current version 22 June 2026.

Digital Object Identifier 10.1109/ACCESS.2026.3696889

RESEARCH ARTICLE

Technical and Economic Feasibility Study of a Grid-Connected Solar Power Plant in Northwest Algeria for Charging Electric Vehicles

GHIZLENE CHEIKH[1], FATIMA BOUTLILIS[2], JÂNIO MONTEIRO[3], CRISTIAN-GYŐZŐ HABA[4], (Member, IEEE), AND HADJ ADDA BENTOUNES[5]

[1]Laboratory of Renewable Energies and Electrical Systems, Laboratory of Signals and Systems, Department of Electrical Engineering, Faculty of Science and Technology, Abdelhamid Ibn Badis University of Mostaganem, Mostaganem 27000, Algeria
[2]Laboratory of Renewable Energies and Electrical Systems, Department of Electrical Engineering, Faculty of Science and Technology, Abdelhamid Ibn Badis University of Mostaganem, Mostaganem 27000, Algeria
[3]Smart and Sustainable Systems Laboratory, Instituto Superior de Engenharia, Universidade do Algarve, Campus da Penha, 8005-139 Faro, Portugal
[4]Department of Electrical Engineering, Gheorghe Asachi Technical University of Iaşi, 700050 Iaşi, Romania
[5]Renewable Energies and Electrical Systems Laboratory (ERSE), CDSEE Laboratory, Department of Electrical Engineering, Faculty of Sciences and Technology, Abdelhamid Ibn Badis University of Mostaganem, Mostaganem 27000, Algeria

Corresponding author: Ghizlene Cheikh (ghizlene.cheikh.etu@univ-mosta.dz)

This work was supported by the by the European Union, under the Programa Operacional de Cooperação Transfronteiriça Espanha-Portugal (POCTEP) and Interregional Cooperation European Territorial Cooperation Programme (INTERREG) programs, in the scope of the projects of Local Energy Communities, Desarrollo de actuaciones piloto para el fomento de comunidades energéticas locales en entornos rurales del espacio POCTEP, CEL-RURAL (0081_CEL_RURAL_6_E_V3) and POCTEP and Almacenamiento y Gestión de Energía Renovable para el fomento de la participación de pequeños y medianos prosumidores en redes eléctricas inteligentes, AGERAR+ (0091_AGERAR_PLUS_6_E).

ABSTRACT The ongoing expansion of electric vehicles requires the development of charging infrastructures, preferentially powered by clean energy sources. This study investigates the optimal design of a hybrid photovoltaic/battery/grid system to supply an electric vehicle charging station in Mesra, Mostaganem province, Algeria. The approach integrates 22 years of high-resolution climate data analysis, the development of a representative charging load profile based on three EV models, and a techno-economic optimization performed with HOMER Pro software. The proposed station is dimensioned to satisfy the expected daily charging load, corresponding to about 97 vehicles per day. Results highlight an optimal configuration combining photovoltaic panels, a battery storage system, and grid backup, ensuring full supply reliability. The energy mix achieves a well-balanced contribution between solar generation, battery storage, and grid electricity. Economic analysis demonstrates strong feasibility, characterized by a highly competitive levelized cost of energy and a reasonable initial investment, confirming the economic attractiveness of the proposed system. From an environmental perspective, the system achieves complete elimination of critical air pollutants and a substantial reduction in CO_2 emissions. This research provides both a scalable framework for integrating renewable energy into EV charging infrastructures and a strategic contribution to Algeria's transition toward a cleaner and more resilient energy mix.

INDEX TERMS Algeria energy transition, electric vehicle charging infrastructure, HOMER pro simulation, renewable energy integration, techno-economic optimization.

I. INTRODUCTION

Renewable energy (RE) represents a key pathway for reducing greenhouse gas (GHG) emissions, decreasing dependence on hydrocarbons, and promoting sustainable electricity generation [1]. Many countries are increasingly investing in clean technologies to strengthen energy security and support long-term economic development. Among them, Algeria endowed with exceptional solar potential exceeding 2,500 hours of sunshine annually, has strong assets for a successful energy transition [2], [3]. Photovoltaic (PV) generation is particularly promising, however, its intermittent

The associate editor coordinating the review of this manuscript and approving it for publication was Katherine VanDenburgh.

nature and reliance on climatic conditions limit its optimal integration, leading most large-scale PV plants in the country to be connected directly to the national grid. Meanwhile, Algeria's continued reliance on hydrocarbons remains a major contributor to GHG emissions, highlighting the urgent need for a more balanced and sustainable energy mix.

In parallel with electricity generation, the transport sector has emerged as another critical contributor to environmental pollution, largely due to the predominance of combustion engine vehicles [4]. The transition to electric vehicles (EVs) is therefore regarded as a relevant global solution for reducing both carbon emissions and noise pollution. Nevertheless, this transition introduces significant challenges, particularly the sharp increase in electricity demand, which requires the development of extensive fast-charging infrastructure [5]. The widespread adoption of EVs is thus closely tied to the availability of charging stations. Currently, most of these stations are supplied by the national grid, thereby reinforcing reliance on fossil fuels [6]. A more sustainable alternative would be to power EV charging stations directly with renewable energy sources (RES), depending on their local availability. Such an approach could simultaneously reduce dependence on hydrocarbons and improve the utilization of renewable resources. However, effective integration requires careful consideration of RE potential particularly solar energy to ensure reliable supply, cost efficiency, and reduced dependence on the central grid.

In this context, and in view of the increasing adoption of EVs in Algeria [7], this work proposes the design and sizing of an EV charging station powered by a hybrid renewable energy system, to be deployed in the village of Mesra, located 13 km south of Mostaganem. This coastal region of northern Algeria benefits from a temperate climate and a favorable solar resource. The primary objective of the proposed system is to ensure a clean, stable, and economically viable electricity supply while reducing dependence on the conventional grid and minimizing CO_2 emissions.

The methodology adopted in this study is structured around the following steps:

- A comprehensive assessment of the climatic characteristics, solar potential, and social-urban constraints of the selected site.
- Analysis of 22 years of local meteorological data, including solar radiation and ambient temperature.

Estimation of energy demand using standardized load profiles for three commonly used EV models.

- Analytical evaluation of the station's daily charging capacity.
- Sizing of the photovoltaic generator and battery-storage subsystem.
- Optimization of the hybrid system using HOMER Pro, through multiple scenario-based simulations to determine the most technically and economically suitable configuration.
- Final evaluation of the system's technical, economic, and environmental performance indicators.

This comprehensive approach enables the identification of the optimal configuration that best aligns with the site's climatic, energetic, and economic characteristics. Overall, the proposed work provides a concrete contribution to the integration of RE into EV charging infrastructure, particularly in rural and semi-urban contexts in Algeria.

The remainder of this paper is structured as follows. Section II presents a focused literature review, summarizing recent studies selected according to defined relevance criteria and analyzing their methodological approaches, contextual relevance, and limitations, while identifying the research gaps that motivate the present study. Section III provides a broad overview of the methodological framework adopted in this study, outlining the key analytical steps, the data sources considered, and the general principles guiding the development of the proposed system. Section IV presents and discusses the obtained results, including the technical performance of the hybrid system, the operational behavior of its major components, the global energy balance, and the associated environmental and economic impacts. Finally, Section V concludes the study by synthesizing its key findings and identifying promising avenues for future research and system enhancement.

II. LITERATURE REVIEW

The EVs have emerged as a crucial pathway for reducing greenhouse gas emissions and improving urban air quality, supported by rapid technological progress and declining battery costs. However, the expansion of EV adoption is still constrained by the need for efficient, reliable, and cost-effective charging infrastructure. Integrating RES into EV charging stations has therefore become a promising strategy to enhance system sustainability, reduce grid stress, and support decentralized clean energy generation.

Despite these advantages, the combination of EV charging and RES also presents notable challenges, including the intermittency of renewable resources, the optimal sizing of hybrid systems, and the need for advanced energy and demand-side management. As a result, recent studies have increasingly focused on analyzing RES-based EV charging solutions both standalone and grid connected to identify effective, context specific configurations that account for climatic conditions, resource availability, and economic constraints.

In this context, [8], the authors conducted a techno-economic evaluation of EV charging stations based on a hybrid PV/WT/battery system across five cities in China using HOMER Pro. The results showed that the hybrid configuration is the most cost-effective solution due to the seasonal complementarity between solar and wind resources, with Nanjing emerging as the most economical site. However, the load profile relies on simplified hypothetical assumptions that do not reflect real charging behavior or demand variability, and the small-scale scope limits its applicability to larger infrastructures. Furthermore, although a sensitivity analysis is included, stochastic modelling of user behavior

TABLE 1. Comparison of the selected studies according to the defined criteria.

Criteria/Study	(2022) [?]	(2022) [?]	(2023) [?]	(2023) [?]	(2024) [?]	(2024) [?]	(2025) [?]	Our Study
RES Integrated	✓	✓	✓		✓	✓	✓	✓
Grid Connection		✓	✓	✓	✓	✓		✓
EV Charging Model	✓	✓	✓	✓	✓		✓	✓
Storage Integration	✓	✓			✓	✓	✓	✓
Long-term Climate Analysis				✓			✓	✓
Optimization Framework	HOMER	Experimental (No optimization)	MATLAB /PVGIS	MATLAB /Simulink	HOMER	HOMER	MFO Metaheuristic	HOMER
Techno-Economic Analysis	✓		✓		✓	✓	✓	✓
Environmental Analysis	✓	✓			✓	✓		✓
Large Scale						✓		✓
Payback		✓			✓	✓	✓	✓
Sustainability	✓	✓			✓	✓		✓
Country	China	France	France	Italy	India	Libya	Greece	Algeria

and renewable generation uncertainty is absent, and the China-specific context restricts the generalization of these findings to other geographical settings.

Similarly, the work presented in [9] experimentally investigated a grid-connected PV/battery/EV microgrid installed at the University Institute of Technology (IUT) in Mulhouse, France. Based on real measurement data, their study focused on optimizing photovoltaic self-consumption and demand management. The system, consisting of two PV subsystems of 2.16 kWp and 2.4 kWp coupled with a lithium-ion storage unit integrated into an EV, proved efficient under real-world operating conditions, achieving a self-consumption rate of nearly 88% on a typical summer day. However, the study is limited to a single EV and two low-capacity PV subsystems with no optimization framework or techno-economic analysis, and the performance evaluation is confined to two arbitrarily selected days without seasonal or long-term assessment, restricting the generalization of these findings to larger or commercially oriented charging infrastructures.

Building on this work, the study presented in [10] proposed a modular PV sizing method for workplace EV charging using six years of empirical data from a French industrial site. By analysing three charging strategies—Plug and Charge, Mean Power, and Solar Smart Charging—the authors showed that strategies improving the alignment between charging demand and solar production can reduce the required PV capacity by 50–70%. However, the approach remains limited to one site and does not account for storage or grid constraints, restricting its applicability to early prefeasibility assessments. Furthermore, the method relies on deterministic charging data and assumes accurate PV generation forecasting, which may not reflect real-world uncertainties. From a theoretical standpoint, the approach remains heuristic and does not rely on a formal optimization or stochastic modeling framework, limiting its ability to ensure optimality and generalize under varying operating conditions.

In addition, another relevant contribution was made by [11], which developed a modular ultra-fast AC/DC optimized charging station capable of reaching 350 kW. Through MATLAB/Simulink simulations, the study achieved a conversion efficiency exceeding 96%, highlighting the importance of advanced converter architectures for high power applications. However, this single-stage architecture, while more efficient, precludes integration with local storage or renewable generation sources via a DC bus, despite their high infrastructure cost and dependence on stable grid conditions. Furthermore, the optimisation criterion is restricted to efficiency alone, as the absence of operational field data prevents any cost-based analysis.

Further contributions confirmed the growing relevance of hybrid solutions. The study in [12] designed a hybrid charging station in Chennai, integrating solar, wind, a diesel generator, and the grid. Their HOMER Grid simulations demonstrated that the optimized system combined low costs with a high share of RE while achieving 83.8 kW charging capacity. However, the approach remains limited to a single location-specific context and assumes flat component costs, reducing its generalisability to other deployment environments. Furthermore, the continued reliance on a diesel generator as a backup source, alongside the absence of any smart charging strategy and the lack of large-scale empirical data validation, represents a notable limitation for fully renewable and demand-responsive deployments.

In the same year, the analysis in [13] assessed a PV/WT/BESS based charging station connected to the grid in Tripoli, Libya. Their results revealed CO_2 reductions of up to 30,472 tonnes per year and greater energy autonomy, although the system faced constraints such as high capital costs and operational complexity. However, the study relies on a short-term location-specific climatic dataset, models EV demand through only two fixed vehicle categories with invariant charging schedules rather than a realistic multi-vehicle profile, and treats the grid as an ideal bus with no network constraints, limiting both the physical representativeness of the simulation and the transferability of the findings to other geographical contexts or larger-scale deployments. Most recently, the authors in [14] studied RE integration into EV charging within a supermarket chain in Crete. Using the Moth–Flame Optimizer (MFO) algorithm, they optimized PV and BESS systems over 20 years, showing PV's high profitability (€6.4 million total profit) while noting that BESS was only beneficial in specific scenarios.

Their recommendation to equip 30% of parking spaces with charging stations, in line with European directives, provides a scalable model for commercial applications.However, the approach relies on a metaheuristic optimization method without guarantees of global optimality and is based on deterministic assumptions. In addition, grid constraints and uncertainties related to EV demand and renewable generation are not explicitly considered. From a theoretical perspective, the lack of uncertainty-aware optimization limits the robustness and generalizability of the results.

To provide a clearer overview of the most relevant recent contributions in this field, Table 1 summarizes the main characteristics, methodologies, and key findings of the reviewed studies. The comparison is structured around key criteria such as system configuration, RES integration, grid connection, EV charging modelling, climatic data analysis, optimization frameworks, and technoeconomic or environmental assessments. This synthesis highlights the growing research interest in renewable based EV charging systems and underlines the diversity of configurations and optimization tools employed worldwide.

Collectively, existing studies demonstrate the technical feasibility and economic potential of RE powered EV charging infrastructures. While these contributions highlight important benefits such as improved service continuity, reduced greenhouse gas emissions, and strengthened integration of RE most remain constrained by site specific assumptions, limited climatic datasets, small system scales, and simplified EV charging behaviors. As a result, their findings often lack transferability to regions with different resource profiles or to projects requiring high reliability and long term economic sustainability.

In contrast, the present study addresses these limitations by proposing a configuration explicitly designed to minimize investment costs, reduce greenhouse gas emissions, and maximize the share of RE, while ensuring high operational reliability. This is achieved through the use of a multidecadal solar resource dataset, enabling a robust assessment of interannual climatic variability, and through the development of a realistic and scalable EV charging profile that can be applied to a variety of regions and infrastructure sizes. Furthermore, by focusing on a country with exceptionally high renewable energy potential, the study leverages abundant solar resources to improve both the financial viability and long term durability of the proposed system.

Through this comprehensive and context adapted approach, the study identifies the configuration that best aligns with the climatic, energetic, and economic characteristics of the target region, thereby offering a reliable and sustainable framework for the large scale deployment of RE based EV charging stations.

III. METHODOLOGY

This section outlines the methodological framework adopted to size and optimize the proposed EV charging station. The system under study is designed as a hybrid configuration that integrates three main components: a PV generator, a BESS, and the connection to the national electricity grid. This combination allows for greater reliability while ensuring optimal exploitation of renewable resources but comes with the inherent complexity of allowing multiple configuration options each one with a different impact in the evaluation parameters.

The rest of this section is organized as follows. First, the characterization of the project site and the analysis of long term climatic data are presented, followed by the estimation of the station's energy requirements and load profile. Next, the architecture of the proposed system is formulated, and the procedures for sizing the photovoltaic generator, the battery storage bank, and the power conditioning units are detailed. Finally, the technical, economic, and environmental indicators adopted for the evaluation and optimization of the system are introduced.

A. PROJECT SITE

The selected site is located at geographical coordinates 35.93° N, 0.09° E. It benefits from substantial solar irradiation throughout the year, as shown in Figure 1.

B. CLIMATE DATA

The climatic data used in this study were obtained from NASA's Surface Meteorology and Solar Energy database [16], covering a 22 year observation period to ensure both representativeness and reliability of the simulations. The dataset provides monthly averages of daily solar radiation (kWh/m^2/day) and ambient temperature (°C), which are illustrated in Figures 2 and 3.

In terms of solar radiation, as illustrated in Figure 2, the site benefits from significant solar potential, with an average annual irradiation of 4.80 kWh/m^2/day. The clearness index remains relatively low during the winter months, ranging from approximately 0.51 to 0.56 (December to February).

Regarding ambient temperature (Figure 3), the site experiences monthly average values ranging from 9.59°C in January to 28.64°C in July. Seasonal variations remain relatively moderate, resulting in an annual average temperature of 18.55°C, which is considered favorable for most environmental and energy related applications.

The climatic analysis, as illustrated in Figures 2 and 3, confirms the suitability of the proposed site for a photovoltaic charging station. The annual solar radiation levels ensure reliable energy generation to meet EV charging demands, while the temperature profile supports efficient photovoltaic performance with minimal losses. In line with existing literature, these results highlight the site's strong potential for photovoltaic deployment, providing a robust basis for a sustainable and self sufficient charging infrastructure tailored to local conditions [17].

C. ESTIMATING ENERGY REQUIREMENTS

Accurate assessment of energy demand is a crucial step in properly sizing an EV charging station. This estimation

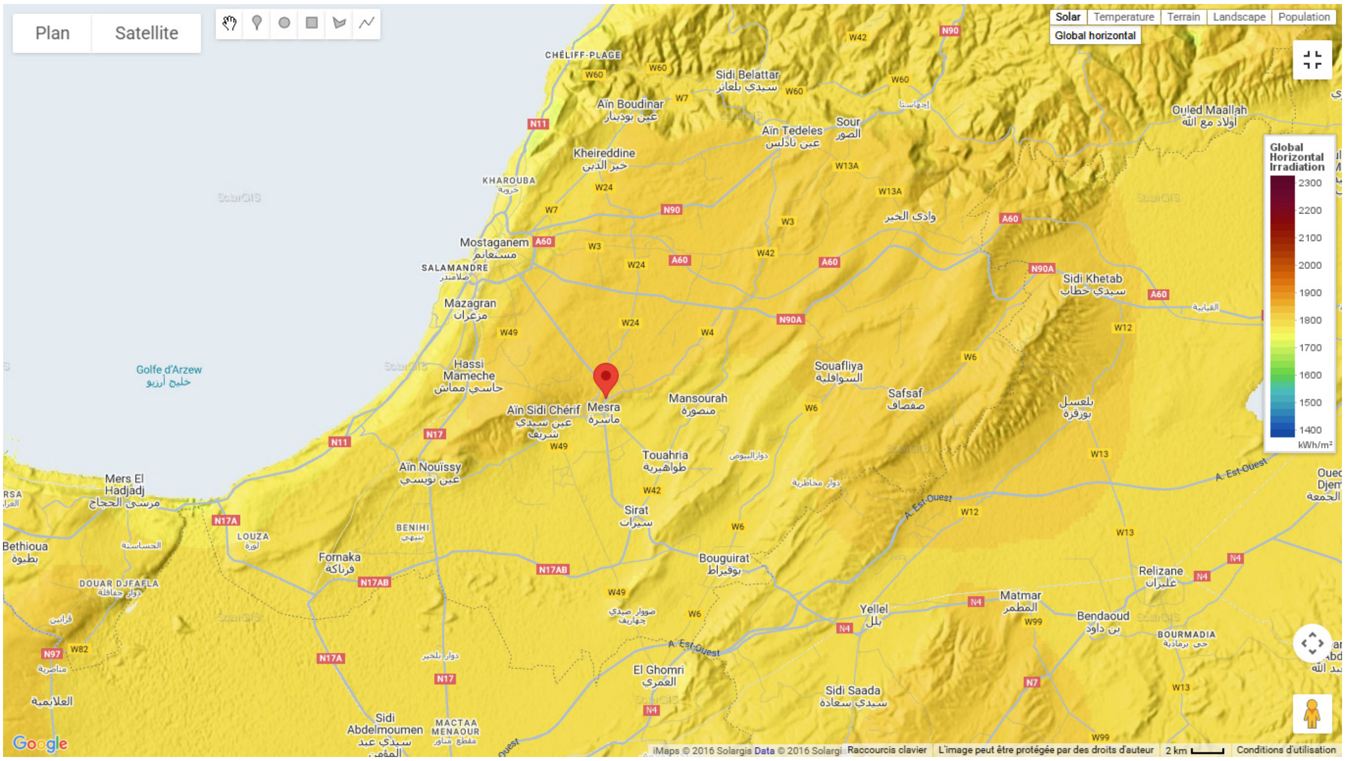

FIGURE 1. Distribution of horizontal global solar radiation in algeria [15].

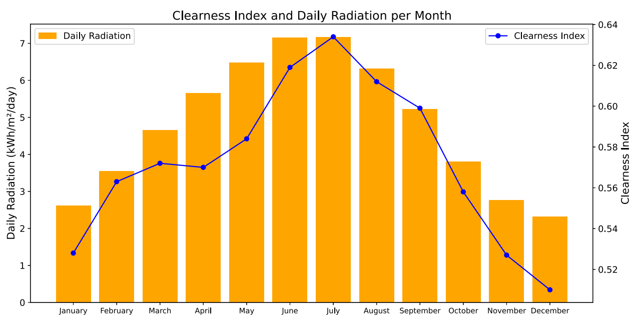

FIGURE 2. Monthly evolution of solar radiation and clearness index.

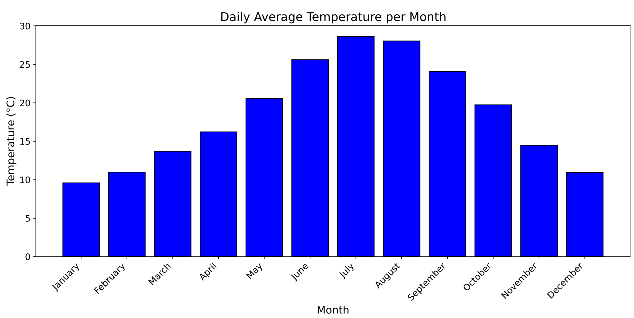

FIGURE 3. Monthly average daily temperatures.

primarily relies on the selection of representative vehicles and a detailed analysis of their charging behavior [18].

1) CHOICE AND CHARACTERISTICS OF EVs

Table 2 presents the specifications and estimated charging times of three representative EV models, reflecting a range of battery capacities and charging powers. This diversity captures the main technological variations among current EVs, thereby enabling a comprehensive assessment of their contribution to overall energy demand.

The charging time of an EV(T_{Ch})in hours is governed by its battery capacity and the power of the charging station. Equation (1) can be approximated by:

$$T_{Ch} = \frac{E_r}{P_b} \tag{1}$$

where:

- E_r: energy to be charged to reach the desired state of charge (kWh),
- P_b: power of the charging station (kW).

This formulation makes it possible to estimate the number of vehicles that can be charged simultaneously and to optimize the selection of charging stations, thereby ensuring a balance between charging speed and the availability of the power infrastructure.

2) STATION CHARGING CAPACITY

T_{Ch} provides the basis for estimating the maximum charging capacity of the station. Following preliminary calculations, the proposed configuration consists of three fast direct current (DC) chargers and two alternating current (AC) chargers,

TABLE 2. Electric vehicle specifications and charging times.

Parameter	Dacia Spring	Tesla Model 3	Renault Zoe
BC (kWh)	26.8	65.0	52.0
$C_{30\%}$ (kWh)	8.04	19.5	15.6
$R_{70\%}$ (kWh)	18.76	45.5	36.4
DC Charging (h)	0.62 (30 kW)	0.18 (250 kW)	0.72 (50 kW)
AC Charging (h)	2.84 (6.6 kW)	4.13 (11 kW)	1.65 (22 kW)

BC: Battery Capacity; $\mathbf{C_{30\%}}$: Capacity at 30%; $\mathbf{R_{70\%}}$: Recharge to 70%.

with an operational period of 21 h per day and an additional 3 h allocated for maintenance.

The daily charging capacity of the station is determined based on the longest charging time observed for DC and AC chargers, defined as (2):

$$T_{\mathrm{Ch,DC}} = \max\left(T^{(i)}_{\mathrm{Ch,DC}}\right),$$
$$T_{\mathrm{Ch,AC}} = \max\left(T^{(i)}_{\mathrm{Ch,AC}}\right) \quad (2)$$

The number of vehicles that can be charged per day is calculated with (3)

$$N = \frac{H \times N_{\mathrm{chargers}}}{T_{\mathrm{Ch}}} \quad (3)$$

where $H = 21$ h is the daily operating time, N_{chargers} is the number of charging points

The resulting daily charging capacity is presented in Table 3. This confirms that the proposed station configuration ensures sufficient capacity while efficiently utilizing the available charging infrastructure.

TABLE 3. Daily charging capacity of the station.

Charger type	N_chargers	Total vehicles (21 h)
Fast chargers (DC)	3	87
Standard chargers (AC)	2	10
Total station (DC+AC)	5	97

3) ESTIMATION OF THE ENERGY CONSUMPTION PROFILE

Following the definition of charging capacity, the station's total daily energy consumption over a 21 hour operating period is estimated. As shown in (6) this value depends on the number of vehicles charged at DC and AC stations (Table 3) and the average energy demand per vehicle. It is expressed as:

$$E_{\mathrm{total}} = (N_{\mathrm{DC}} + N_{\mathrm{AC}}) \times E_{\mathrm{avg}} \quad (4)$$

where the average energy per vehicle is defined (5) as:

$$E_{\mathrm{avg}} = \frac{\sum_{i=1}^{n} E_{r_i}}{n} \quad (5)$$

with E_{r_i} representing the recharged energy of vehicle i, and n being the total number of considered vehicles.

Substituting the computed parameters into (4), the total estimated average daily energy consumption is obtained as:

$$E_{\mathrm{total}} = 3254.5 \text{ kWh} \quad (6)$$

The corresponding hourly demand profile is shown in Figure 4, which highlights the temporal variation in energy use throughout the day.

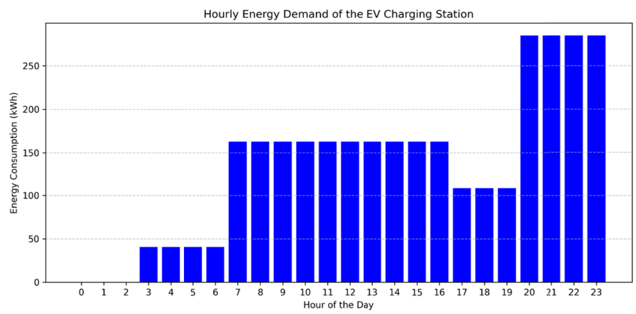

FIGURE 4. Hourly energy demand of the EV charging station.

The load profile exhibits four distinct periods and closely resembles a typical residential demand pattern, with peak consumption occurring between 7:00 a.m. and 4:00 p.m. Based on these results and the estimated load profile, an optimal station configuration and energy management approach can be proposed, incorporating renewable energy sources. The hourly load profile was developed using a structured station-level modelling methodology based on representative EV types and their corresponding charging energy requirements. After estimating the total daily demand, the energy was distributed into an hourly load curve through a rule-based synthesis approach, assigning predefined percentages to different periods of the day. This distribution includes negligible nighttime demand, limited early-morning activity (5%), increased morning charging (25%), moderate daytime demand (20%), a pronounced evening peak (40%), and reduced late-evening demand (10%). This formulation ensures a smooth and representative daily charging pattern while providing a consistent and computationally efficient input for system sizing, optimization, and energy management analyses.

D. PROPOSED CONFIGURATION

Figure 5 presents the proposed hybrid architecture supplying the EV charging station. The system is structured around two coordinated buses: an AC bus connected to the grid and a high voltage DC bus (974 V) linking the renewable energy source, the battery storage system, and the EV chargers. The grid is interfaced with the DC bus through a bidirectional AC/DC converter, which allows both importing energy during periods of low renewable production and exporting excess energy when available. The renewable source which is a photovoltaic array is connected via an MPPT-controlled DC/DC converter to ensure maximum power extraction under varying environmental conditions. A bidirectional DC/DC converter also couples the battery storage to the DC bus, managing charge–discharge operations, stabilizing the DC bus voltage, and supporting rapid load fluctuations during EV fast charging. The EV charging stations are interfaced

TABLE 4. Monthly global irradiation and number of equivalent sun hours in Mesra[21]).

Season / Month		Winter			Spring			Summer			Autumn	
Month	Jan	Feb	Mar	Apr	May	Jun	Jul	Aug	Sep	Oct	Nov	Dec
Irradiation E_{sol} (Wh/m^2/day)	2610	3540	4650	5650	6480	7150	7160	6310	5220	3800	2760	2310
Sun hours N_e (h/day)	2.61	3.54	4.65	5.65	6.48	7.15	7.16	6.31	5.22	3.80	2.76	2.31

with the DC bus through an appropriate DC/DC conversion stage to ensure voltage regulation and safe charging operation. This architecture ensures flexible energy management, allowing the renewable source to supply the load when available, the battery to smooth power fluctuations or provide support, and the grid to act as a backup source during periods of low renewable generation or low battery state of charge.

E. SIZING OF THE PHOTOVOLTAIC (PV) GENERATOR

The design of a photovoltaic system requires optimizing the configuration of its components to ensure a reliable energy supply. This process begins with the assessment of the station's daily energy demand, followed by an analysis of local solar conditions (irradiation, orientation, and panel slope) [19]. Based on these parameters, the required PV peak power is determined, accounting for losses from converters, cabling, temperature, and other operational factors. Appropriate converters and storage devices are also integrated to ensure continuous supply despite solar intermittency.

1) MODULE ORIENTATION AND INCLINATION

Maximum energy yield is obtained when modules are oriented perpendicular to incoming solar radiation [20]. For the studied site, optimal conditions are achieved with a inclination angle of 33° and an azimuth of 4°, ensuring efficient annual energy capture without the need for tracking systems.

2) DAILY ELECTRICAL PRODUCTION OF A SINGLE MODULE

The daily output of a photovoltaic module is estimated using the concept of equivalent sun hours (N_e), in hour/day, which correspond to the integrated solar energy received under a standard irradiance of 1000 W/m^2 [21]. This allows estimating the daily solar energy per unit surface area (E_{sol}), expressed in Wh/m^2/day, using (7):

$$E_{\text{sol}} = N_e \times 1000 \tag{7}$$

To characterise the solar resource at the chosen site, Table 4 reports the monthly averages of irradiation and equivalent sun hours, providing a reliable basis for estimating photovoltaic potential and system sizing [21].

3) ELECTRICAL LOSSES

In photovoltaic (PV) systems, electrical and environmental losses represent an inherent and unavoidable aspect of energy conversion. These losses arise at different stages of the system from the PV modules to the inverter and distribution network—and must be carefully accounted for during the design process. Neglecting these effects would lead to an overestimation of the available energy and, consequently, an undersized generator.

Generally, the rate of each loss is specified or can be derived from the technical data sheets of the system components. For instance, inverter efficiency, cable resistivity, and module temperature coefficients are provided by manufacturers, while other losses, such as those due to soiling or low irradiance, are estimated empirically based on site conditions and operating experience [22].

To reflect these effects accurately, standard loss factors typically considered in PV design are summarized in Table 5. These values are consistent with the performance assumptions used in PVsyst and other professional simulation tools, ensuring a realistic estimation of the system's net energy output. The adopted loss coefficients are based on standard installation guidelines and widely accepted design practices in the PV industry [23], where each factor represents typical operating conditions and provides a practical approximation of real-world system performance.

TABLE 5. Loss coefficients in the photovoltaic energy system [22].

Designation	% Losses	Efficiency (%)
Inverter losses	10	90
Temperature losses	10	90
Cable and connection losses	3	97
Losses due to soiling	10	90
Low irradiation losses	4	96
Module quality losses	3	97

4) LOSS COEFFICIENT EVALUATION (C_p)

The overall DC side efficiency of the photovoltaic field is represented by a global loss coefficient, C_p, obtained by multiplying the partial efficiencies of each subsystem. The values used in (8) are taken directly from Table 5.

$$C_p = 0.9 \times 0.9 \times 0.97 \times 0.90 \times 0.96 \times 0.97 \tag{8}$$

which gives (9):

$$C_p = 0.65 \quad (65\%) \tag{9}$$

This coefficient represents the cumulative impact of environmental and electrical losses—such as temperature effects, soiling, and cabling—on the energy produced by the PV array before AC conversion. It ensures that the array is dimensioned based on realistic operational conditions rather than ideal ones.

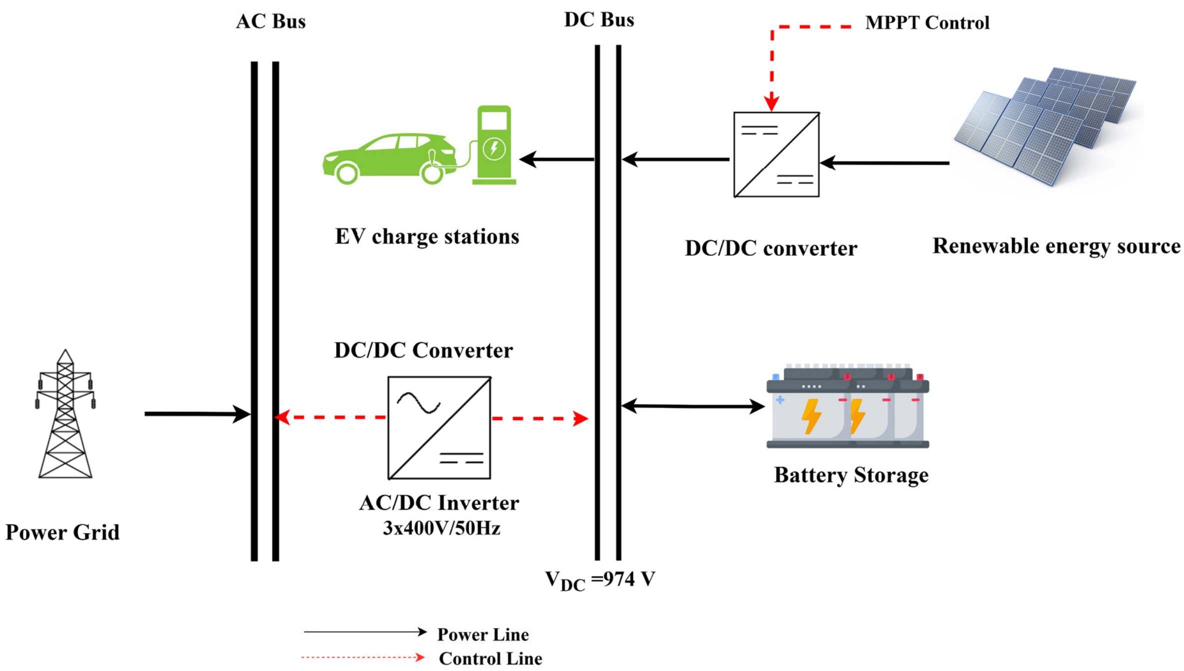

FIGURE 5. General configuration of the proposed hybrid electrical system.

5) PHOTOVOLTAIC ARRAY DESIGN

The PV array is sized according to the station's peak power requirement, constrained by inverter input voltage for series connections and input current for parallel connections [24]. The required PV capacity is calculated as show in (10) and (11):

$$P_{PV} = \frac{E_{load}}{\eta_{sys} \cdot G_{sol}} \tag{10}$$

where:

- E_{load} is the daily energy consumption of the station (kWh/day),
- $G_{sol} = 4.8$ kWh/m^2/day is the mean daily solar irradiation of chosen site,
- $\eta_{sys} = 0.8$ represents: global system efficiency.

$$P_{PV} = 847.5 \text{ kW} \tag{11}$$

The number of modules is determined by (12):

$$N_{PV} = \frac{P_{PV}}{P_{module}} \tag{12}$$

For the considered modules, this corresponds to (13):

$$N_{PV} \approx 2457 \text{ to } 2690 \tag{13}$$

where P_{module} is the peak power of the selected Trina Solar polycrystalline module (345 W or 315 W [25]).

F. INVERTER ADAPTATION

The power rating of the inverter must comply with the following empirical condition [26] as expressed in (14):

$$0.8 \leq \frac{P_{inv,max}}{P_{installed}} \leq 1.2 \tag{14}$$

In this work, the Eaton Power Xpert 1000 kW inverter was selected, with its technical specifications detailed in [27]. Verification of (14) confirms the validity of this choice, as result in (15):

$$\frac{P_{inv,max}}{P_{installed}} = \frac{1000}{847.5} = 1.17 \tag{15}$$

where $P_{inv,max}$ is the maximum inverter power and $P_{installed}$ is the installed PV capacity. The obtained ratio lies within the recommended range (0.8–1.2), ensuring the compatibility of the inverter with the system.

1) MAXIMUM NUMBER OF SERIES CONNECTED MODULES

The number of modules connected in series is limited by the inverter's admissible DC input voltage range (750–1250 V [27]). Equation (16) defines the maximum number of series modules:

$$N_s = \frac{U_{inv,max}}{V_{oc}} \tag{16}$$

where $V_{oc} = 46.4$ V (open-circuit voltage of the module) and $U_{inv,max} = 1250$ V (maximum DC input voltage of the inverter). The allowable range lies between 17 and 26 modules in series.

2) NUMBER OF PARALLEL STRINGS

For $N_{PV} = 2457$ modules, the number of parallel strings is (17):

$$N_{ps} = \frac{N_{PV}}{N_s} \tag{17}$$

The maximum input current is given by (18):

$$I_{max} = N_{ps} \times I_{sc} \tag{18}$$

where $I_{sc} = 9.62$ A (module short circuit current), and the inverter maximum input current is limited to 1816 A.

Table 6 indicates that the optimal PV configuration consists of 21 modules in series and 117 parallel strings, yielding 974.4 V and 1126.5 A. These values remain within the inverter's operating limits (1250 V and 1816 A), providing a peak power of 847.7 kWp. This configuration ensures compliance with technical constraints while guaranteeing reliable and efficient energy supply for the charging station.

TABLE 6. Possible configurations of the PV generator.

N_s	U_{DC} (V)	N_{ps}	I_{max} (A)	N_{tpv}	P_t (W)
26	1206.4	94	904.3	2444	842220
25	1160.0	98	942.8	2450	845250
24	1113.6	102	981.2	2448	844560
23	1067.2	106	1019.7	2438	841110
22	1020.8	111	1067.8	2442	843490
21 (Optimal)	**974.4**	**117**	**1126.5**	**2457**	**847665**
20	928.0	122	1174.6	2440	841800
19	881.6	129	1243.0	2451	846595
18	835.2	136	1308.3	2448	844560
17	788.8	144	1385.3	2448	844560

N_s: modules in series; U_{DC}: DC voltage; N_{ps}: parallel strings; I_{max}: maximum current; N_{tpv}: total number of modules; P_t: total power.

G. DC/DC CONVERTER AND MPPT ADAPTATION

Following the inverter adaptation, a DC/DC converter is implemented to ensure proper voltage regulation between the PV array and the inverter. Its main function is to stabilize the DC bus voltage and to enable the PV generator to operate continuously at its Maximum Power Point (MPP), regardless of changes in solar irradiance and temperature.

The converter integrates an MPPT control algorithm that dynamically adjusts the operating point of the PV modules to extract maximum available power. In this system, the PV field provides an installed capacity of 847.5 kW, consisting of approximately 2,457 Trina Solar polycrystalline modules rated at 345 W each. Each module operates at 37.7 V and 9.15 A, resulting in a string voltage of about 974 V for 21 modules in series. The converter's MPPT voltage range of 64–1300 VDC ensures full compatibility with this configuration, guaranteeing efficient power transfer and stable operation of the photovoltaic charging system.

H. SIZING OF THE STORAGE SYSTEM (BATTERY)

The storage system plays a crucial role in ensuring the continuity of energy supply and in maximising the share of solar self consumption [28]. Its required capacity is

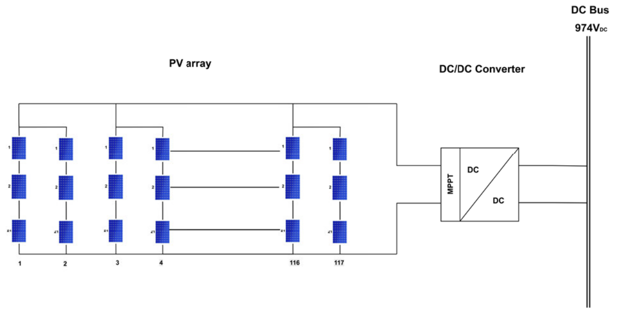

FIGURE 6. Photovoltaic array configuration (P_V = 847.5 kW, 2,457 modules, 21S × 117P).

determined from the station's daily energy demand E_{conso} and the desired autonomy period $j_{auto} = 1$, according to 19:

$$E_{stock} = E_{conso} \times j_{auto} \tag{19}$$

The corresponding storage bank capacity C_{bat}, expressed in ampere hours, is then derived from the system voltage V_{bat}, the permissible depth of discharge (DoD), and the efficiency factor ρ of the selected storage technology [29], as refer in 20:

$$C_{bat} = \frac{E_{stock}}{V_{bat} \times \text{DoD} \times \rho} \tag{20}$$

The number of batteries required is calculated from the unit capacity of each module C_{unit}, as expressed in 21:

$$N_{bat} = \frac{C_{bat}}{C_{unit}} \tag{21}$$

For this study, the Discover AES 6.6 kWh – 48Vdc battery was selected(). With a unit capacity of 130 Ah [30], the system requires approximately 685 batteries, arranged in 20 series and 35 strings connected in parallel to achieve voltage compatibility with the system's DC bus ($U_{DC} \approx 974, 4$ V). This configuration ensures both the required storage capacity and operational compatibility of the charging station.

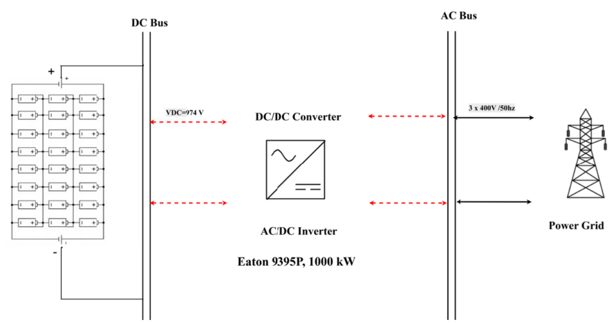

FIGURE 7. Schematic diagram of the Discover AES 6.6 kWh battery bank(20S × 35P = 700 units, 974.4 V DC).

In the proposed system, the central electricity grid functions as a supplementary source of energy, ensuring continuous supply when solar generation and storage are insufficient. This backup role is particularly relevant during

TABLE 7. Economic indicators of grid exchanges [32].

Parameter	Value
Grid power purchase price	0.060 €/kWh
Grid sellback price	0.055 €/kWh
Net purchases calculation	Monthly

periods of reduced solar availability or peak demand. The associated economic parameters of grid utilization are presented in Table 7 [31].

This section confirms the technical feasibility of a hybrid clean energy system for the charging station. The sizing of photovoltaic modules, storage, converters, and grid integration ensures both reliability and operational continuity. The proposed design enhances system autonomy while increasing the contribution of RE, thereby improving overall efficiency and sustainability. These outcomes provide a solid foundation for subsequent simulation and performance evaluation.

I. TECHNICAL AND ECONOMIC INDICATORS

The evaluation of a hybrid multi source energy system requires both technical and economic assessment, with emphasis on cost effectiveness, reliability, and long term performance. Key parameters include production costs, service continuity, and grid dependency, supported by extended technical and financial data.

1) NET PRESENT COST (NPC)

The Net Present Cost (NPC) represents the total life cycle cost of the system. It encompasses the initial capital investment, component replacement costs, operation and maintenance expenses, as well as potential revenues, all discounted over the project's lifetime [33]. Equation 22 presents the computational formulation:

$$NPC = \frac{C_{ACC} + C_{ARC} + C_{AOM}}{CRF(i, n)} \tag{22}$$

where:

- C_{ACC}: annualized capital cost,
- C_{ARC}: annualized replacement cost,
- C_{AOM}: annual operation and maintenance cost,
- $CRF(i, n)$: capital recovery factor,
- i: discount rate,
- n:project lifetime (years).

With, the Capital Recovery Factor (CRF) is defined as 23:

$$CRF(i, n) = \frac{i(1+i)^n}{(1+i)^n - 1} \tag{23}$$

This formulation allows system costs to be expressed in present value, thereby providing a robust basis for economic performance comparison.

2) COST OF ENERGY (COE)

The Cost of Energy (COE) quantifies the average cost of electricity produced by the system over its lifetime, expressed in €/kWh. It incorporates capital investment, replacement costs, and operation and maintenance expenses, and is defined as 24, [34]:

$$COE = \frac{C_{ACC} + C_{ARC} + C_{AOM}}{E_{annual}} \tag{24}$$

where E_{annual} is the annual energy supplied by the system (kWh/year).

This indicator enables direct comparison between the cost of electricity from the hybrid system and that of the conventional grid, thus serving as a key measure of economic competitiveness.

3) LOSS OF POWER SUPPLY PROBABILITY (LPSP)

The Loss of Power Supply Probability (LPSP) is a reliability indicator that measures the proportion of energy demand not met by the system. It is expressed as the ratio of the total unmet demand to the overall load requirement over the study period [35], as expressed in 25:

$$LPSP = \frac{\sum_{t=1}^{T} E_{deficit}(t)}{\sum_{t=1}^{T} E_{load}(t)} \times 100\% \tag{25}$$

where: $E_{deficit}(t)$ = energy deficit at time t (kWh).
$E_{load}(t)$ = load demand at time t (kWh).
T = total number of time periods considered.

4) SELF CONSUMPTION (SC)

The Self Consumption index (SC) quantifies the fraction of locally generated photovoltaic energy that is directly used to supply the load. It is expressed as [36], 26:

$$SC = \frac{E_{PV,local}}{E_{PV,tot}} \tag{26}$$

where:

- $E_{PV,local}$ is the PV energy directly consumed by the load (kWh/year),
- $E_{PV,tot}$ is the total photovoltaic energy production (kWh/year).

This indicator reflects the degree to which the generated solar energy is locally utilized before being stored or exported. A high SC value indicates efficient local use of renewable energy.

5) SELF SUFFICIENCY (SS)

The Self Sufficiency ratio (SS) measures the share of the total load demand that is supplied by renewable energy sources and storage, without relying on the electrical grid [36]. It is defined in 27:

$$SS = \frac{E_{ren,load}}{E_{load}} \tag{27}$$

where:

- $E_{ren,load}$ is the renewable energy (PV + storage) delivered to the load (kWh/year),
- E_{load} is the total annual load demand (kWh/year).

This indicator describes the level of energy autonomy of the system. A higher SS value corresponds to a stronger independence from the grid.

J. HYBRID SYSTEM DESIGN AND OPTIMIZATION STRATEGY

After sizing the different subsystems, it is essential to structure the design process in a coherent manner to guarantee the overall consistency of the system. Figure 8 presents the flowchart of the adopted methodology, outlining the main steps from identifying the EV load profile to conducting the final technical and economic evaluation.

The adopted strategy relies on an integrated approach that combines modelling, simulation, and optimisation. This was carried out using the HOMER (Hybrid Optimisation Model for Electric Renewables) [37] software developed by National Renewable Energy Laboratory (NREL), which is recognised as a benchmark tool for the assessment of hybrid energy systems. HOMER enables the comparison of multiple system configurations combining renewable generation, battery storage, and the electricity grid. The objective is to determine the optimal balance between energy performance, technical feasibility, and economic viability.

In HOMER, the optimisation process follows an exhaustive search strategy. Based on the component sizes defined by the user, the software generates all feasible system configurations and performs a detailed hourly simulation over an entire year for each candidate system. For every time step, HOMER solves the power balance, manages the charging and discharging of the storage system, and determines whether the grid or backup sources must be used. At the end of each annual simulation, HOMER computes key indicators such as the NPC, COE, and reliability metrics.In HOMER Pro, the reported COE is based on annualized system costs and energy production, and can therefore be considered equivalent to the Levelized Cost of Energy (LCOE) All configurations are then ranked according to their economic performance, with the optimal solution being the one achieving the minimum NPC.

Furthermore, system losses in the simulation are represented using simplified modelling assumptions commonly adopted in system-level energy assessments. Converter losses are modelled using constant efficiency values, while photovoltaic performance is adjusted through a fixed derating factor to reflect real operating conditions [38]. This factor accounts for various degradation effects, including electrical losses and environmental influences such as soiling, shading, and aging [39]. This simplified approach is widely adopted in hybrid energy system studies, as it ensures computational efficiency while maintaining an acceptable level of accuracy at the system scale. Consequently, this procedure enables a comprehensive exploration of the solution space and ensures the identification of the most cost-effective and reliable hybrid system configuration.

K. OPTIMAL CONFIGURATION

Following the simulation process, HOMER identified the optimal hybrid system configuration by jointly considering technical feasibility and economic performance. The resulting architecture integrates photovoltaic generation, battery storage, and grid support, ensuring a balanced and reliable energy supply throughout the project's lifetime. The system was designed around a central DC bus, which interconnects the PV array and the battery bank before conversion to the AC grid.

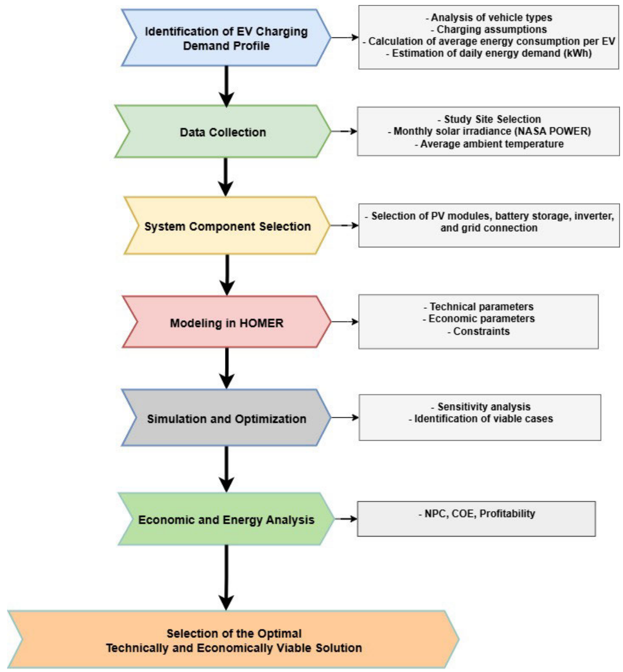

FIGURE 8. Flowchart of the proposed methodology for EV charging system design.

In this configuration, the total charging demand derived from the modeled load profile—encompassing both AC and DC charging points—was represented as an equivalent DC load within HOMER. This modeling approach is justified by the system's DC-coupled architecture, where the majority of power exchanges occur on the DC side. The AC interface is treated through converter efficiency parameters, allowing the model to account for conversion losses implicitly. Representing the global demand as a unified DC load simplifies the optimization process while maintaining physical accuracy. Moreover, this assumption aligns with real world fast charging infrastructures, which increasingly adopt DC-based power distribution to enhance overall system efficiency and minimize conversion losses.

L. OPERATING MODES OF THE HYBRID SYSTEM

Prior to conducting the energy analysis, it is essential to define the hybrid system's operational behavior under varying solar resource conditions and battery states of charge. Two principal modes of operation can be identified:

1) MODE 1: PRIMARY SOURCE–PHOTOVOLTAIC GENERATION AND GRID INJECTION

When the available solar energy exceeds the load demand, the system first checks the battery's state of charge.If the battery is discharged or partially charged, the excess photovoltaic energy is used simultaneously to supply the load and recharge the battery. However, once the battery reaches its full capacity, the surplus solar power is converted into alternating current (AC) and injected into the electrical grid. During this operating mode, the system is primarily powered by the photovoltaic source, ensuring optimal self consumption and effective utilization of surplus energy through grid injection.

2) MODE 2:SECONDARY SOURCE–COMBINED OPERATION OF PV, BATTERY, AND ELECTRICAL GRID

When solar generation becomes insufficient to meet the load demand, the system switches to a hybrid combined mode in which the photovoltaic array, the battery, and the electrical grid work together to ensure a continuous power supply. Initially, the battery discharges to compensate for the lack of photovoltaic production and maintain the supply to the DC load. If the stored energy in the battery becomes insufficient or if the demand exceeds its discharge capacity, the electrical grid automatically intervenes to provide the required supplementary power. This coordinated operation between PV, battery, and grid ensures a stable and reliable energy supply, while optimizing local self consumption and minimizing the system's dependency on the grid.

IV. RESULTS AND DISCUSSION

This section presents and analyzes the results obtained from the simulation of the proposed hybrid RE system for the EV charging station using the HOMER Pro software. The analysis focuses on both technical and economic performance indicators in order to evaluate the system's efficiency, reliability, and contribution to RE integration. The simulation outcomes are organized into several parts: first, the technical performance is examined through the distribution of annual energy production and consumption; second, the economic and environmental aspects are discussed to assess the overall sustainability and feasibility of the proposed configuration.

A. TECHNICAL ANALYSIS OF THE SYSTEM

1) ANNUAL PRODUCTION DISTRIBUTION

The annual energy distribution of the optimal hybrid configuration for the EV charging station is shown in Figure 9. The photovoltaic generation ($E_{PV,tot}$) emerges as the predominant source, particularly between April and August, when solar irradiance is at its peak. The grid import ($E_{purchases}$) is limited to periods of reduced solar availability, primarily in winter months.

As reported in Table 8, the total annual energy production reaches 1,792,485 kWh. The photovoltaic generation ($E_{PV,tot} = 1,330,635$ kWh) contributes the largest share (74.2%).This highlights the dominant role of photovoltaic generation in supplying the system and reducing dependence on the utility grid. Grid electricity purchases amount to $E_{purchases} = 461,850$ kWh, representing 25.8% of the total energy supply. The grid therefore serves as a complementary

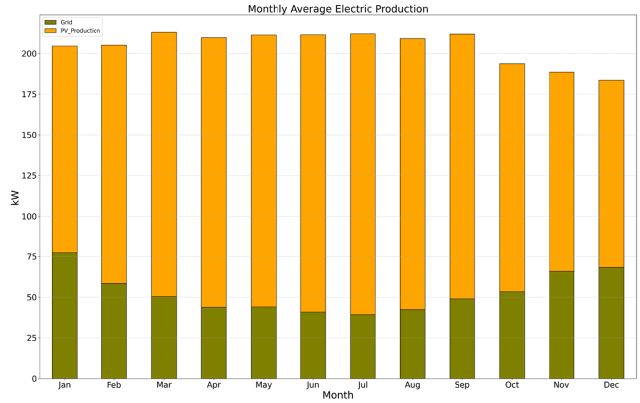

FIGURE 9. Average monthly power generation from $E_{PV,tot}$ and $E_{purchases}$.

energy source, supplying electricity primarily when photovoltaic generation and stored energy are insufficient.

TABLE 8. Annual energy contribution by source.

Energy source	Energy (kWh/year)	Percentage (%)
$E_{PV,tot}$	1,330,635	74.2
$E_{purchases}$	461,850	25.8
Total	1,792,485	100

The system configuration emphasizes the predominance of photovoltaic generation as the primary energy source, while grid imports act as a backup to ensure supply reliability. This hybrid architecture reduces grid dependency and supports the sustainability objectives of the EV charging infrastructure.

2) ANNUAL CONSUMPTION

Table 9 summarizes the system's annual energy consumption. The total production reached 1,673,878 kWh, of which 1,187,881 kWh (71.5%) was consumed by the DC primary load, while 485,996 kWh (29%) was exported to the public grid.

These results indicate that the majority of the generated energy is directly utilized to supply the DC load, while the excess production is exported to the grid. This energy balance reflects an efficient utilization of photovoltaic generation and contributes to improving the overall economic performance of the system.

3) RELIABILITY ASSESSMENT

Table 10 summarizes the reliability indicators of the hybrid system supplying the DC charging infrastructure. One of the key reliability metrics is the unmet electric load, denoted as E_{unmet}, which represents the amount of electrical energy demand that cannot be satisfied by the system over a given period. The system demonstrates excellent operational robustness: E_{unmet} is 0 kWh/year (0%), indicating that the total energy required by EVs is met either from the grid or from solar PV. Similarly,the capacity shortage, represented by E_{shortage}, also remains null, confirming that the installed

TABLE 9. Annual energy consumption.

Consumption	Energy (kWh/year)	Percentage (%)
$E_{\text{Load,DC}}$	1,187,881	71
$E_{\text{Grid,export}}$	485,996	28.9
Total	1,673,878	100

system capacity is sufficient to meet power demand at all times, including during peak load conditions.

TABLE 10. Annual technical reliability criteria of the system.

Quantity	kWh/year	%
Excess Electricity (E_{excess})	83,192	4.64
Unmet Electric Load (E_{unmet})	0	0.00
Capacity Shortage (E_{shortage})	0	0.00

In addition, the system generated an excess electricity flow E_{excess} of 83,192 kWh/year, corresponding to 4.64% of the total energy production. This limited surplus reflects a well-calibrated system design that ensures high operational flexibility while minimizing unused energy. Overall, the absence of unmet electric load and capacity shortage results in a LPSP equal to zero, confirming the high reliability of the proposed hybrid system and its suitability for continuous, stable, and sustainable operation of DC fast charging infrastructure.

Furthermore, Table 11 highlights the RE of the system. A renewable fraction of $f_{\text{ren}} = 72.4\%$ and a maximum renewable penetration of $P_{\text{ren,max}} = 302\%$ were achieved, indicating that, during certain periods, the photovoltaic energy production $E_{\text{PV,total}}$ exceeded the total electrical demand $E_{\text{Load,DC}}$ by more than three times. This significant renewable contribution demonstrates the system's strong reliance on clean energy sources and its ability to supply a substantial portion of the load through renewable generation.

TABLE 11. Renewable energy penetration performance.

Metric	Value (%)
Renewable Fraction (f_{ren})	72.4
Maximum Renewable Penetration ($P_{\text{ren,max}}$)	302.0

Complementary energy based indicators extracted from HOMER are summarized in Table 12. These indicators provide insight into the renewable contribution, energy autonomy, and local utilization of the PV–battery subsystem.

TABLE 12. Key energy based performance indicators.

Indicator	Value (%)
Renewable share in total generation ($E_{\text{ren}}/E_{\text{gen}}$)	79.6
Renewable contribution to load ($E_{\text{ren}}/E_{\text{load}}$)	74.2
Nonrenewable contribution ($(1 - E_{\text{non-ren}})/E_{\text{load}}$)	100

The renewable penetration of 79.6% indicates that a large share of the total energy generation originates from renewable sources, although a noticeable contribution from the grid remains necessary. The SS ratio of 74.2% shows that a substantial portion of the station's annual energy demand is supplied by PV generation and battery discharge, while the grid provides complementary support during periods of insufficient renewable availability. In parallel, the SC rate, computed using HOMER energy balances as 28:

$$SC = \frac{E_{\text{PV,local}}}{E_{\text{PV,tot}}} = \frac{785{,}593}{1{,}330{,}635} \approx 0,5903\ (59.03\%), \quad (28)$$

indicates that more than half of the PV energy is consumed locally, while the remaining fraction is exported to the grid or curtailed. These results confirm that the hybrid PV-battery-grid architecture maintains a significant level of renewable penetration, a moderate degree of self sufficiency, and improved local energy utilization, which are key attributes for sustainable EV charging infrastructure.

B. BEHAVIOR OF THE MAIN SYSTEM COMPONENTS

1) PHOTOVOLTAIC GENERATOR

The PV generator's performance, illustrated in Figure 10, highlights pronounced day to day variability in photovoltaic production during December. The power output exhibits a typical diurnal pattern, with daytime peaks generally ranging between 500 and 750 kW, while nighttime production remains null. Several days show reduced peak levels or shorter production durations, reflecting the strong influence of winter meteorological conditions such as cloud cover and reduced solar irradiance.

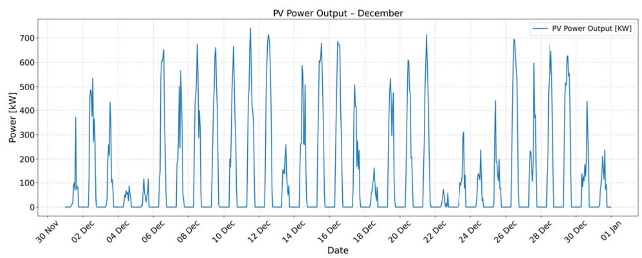

FIGURE 10. PV production power during December.

The photovoltaic power output over the 48 hour period in December exhibits a pronounced diurnal pattern, with near nominal power levels observed around midday on December 15 and 16, indicating effective MPPT operation under favorable irradiance conditions. PV generation drops to zero during nighttime hours and resumes after sunrise on December 17. This behavior confirms the strong dependence of PV production on solar availability and highlights the necessity of energy storage and/or grid support to ensure a reliable supply for EV charging

Furthermore, Figure 12, which illustrates the annual hourly distribution of photovoltaic power output, clearly highlights the seasonal variability of PV generation. Electricity production is primarily concentrated between 08:00 and 18:00, with higher intensity and greater temporal stability observed

TABLE 13. Summary of PV generator performance, annual electrical balance, and economic parameters.

Production Metrics	Quantity	Production Metrics	Quantity
Rated Capacity	848 kW	Average Power	152 kW
Mean Daily Output	3646 kWh/day	Capacity Factor	17.9%
Total PV Production ($E_{\mathrm{PV,total}}$)	1,330,635 kWh	Minimum Power	0 kW
Maximum Power	832 kW	PV Penetration ($P_{\mathrm{PV,pen}}$)	112%
Operating Hours	4,387 h/year	$\mathrm{LCOE_{PV}}$	€0.0649/kWh
Economic Parameters (per kW of installed PV)			
Installed Capacity	1 kW	Capital Cost	€400
Replacement Cost	€300	O&M Cost	€10/year

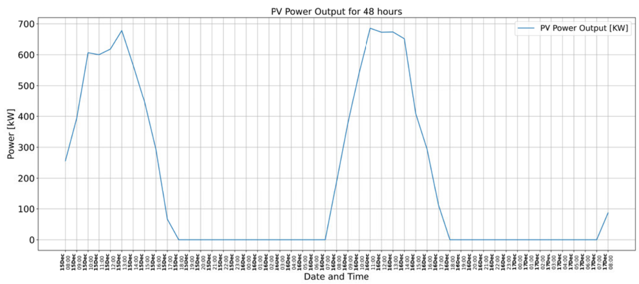

FIGURE 11. Zoomed PV production power for three days (December 15–17).

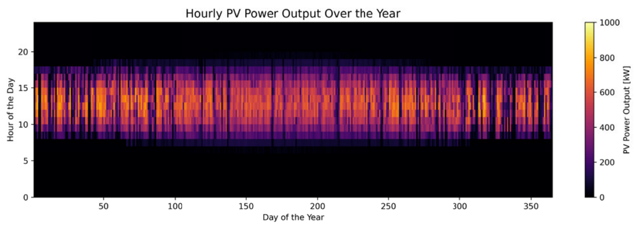

FIGURE 12. Annual DMAP of hourly PV output power.

during spring and summer months. In contrast, winter PV generation is characterized by a reduced daily duration (approximately 6–8 hours) and increased variability due to prevailing weather conditions.

As summarized in Table 13, the photovoltaic generator achieves a total annual energy production of 1,330,635 kWh, with a rated capacity of 848 kW and an average power output of 152 kW(considering night time periods). The system delivers a mean daily energy production of 3,646 kWh/day, corresponding to a capacity factor of 17.9% and approximately 4,387 operating hours per year, which indicates effective utilization of the available solar resource.

From an economic perspective, the levelized cost of energy (LCOE) is estimated at €0.0649/kWh, confirming the economic competitiveness of the PV system. Moreover, the high PV penetration rate of 112% demonstrates the system's ability to meet and exceed local energy demand, thereby enhancing energy autonomy and enabling surplus energy to be allocated to storage systems or additional loads.

2) STORAGE SYSTEM

Figures 13 and 14 illustrate the charging and discharging dynamics of the storage subsystem in December. A clear

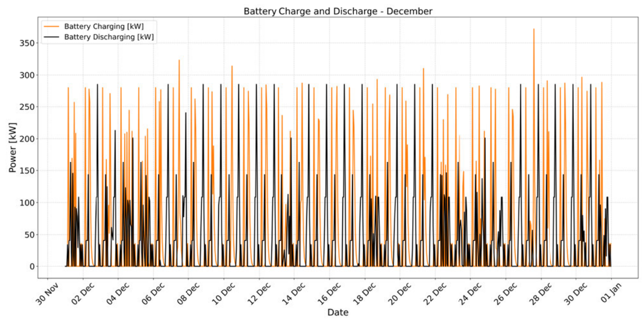

FIGURE 13. Temporal evolution of battery charging and discharging during December.

daily cycling pattern is observed: the battery exhibits multiple charge discharge alternations throughout each day, with peak power levels reaching approximately 280 kW for charging (typically during daytime hours) and 280-290 kW for discharging (concentrated in evening periods). Both phases display characteristic power profiles, reflecting the regulated behavior of the DC/DC converter and the response to variable renewable generation and EV load on the DC bus.

The zoomed 48 hours view reveals that charging occurs primarily during mid-morning to early afternoon, aligned with solar availability, while discharging shows a dual mode behavior with sustained plateaus around 110 kW and brief peaks during demand response events. Overall, the battery exhibits efficient cycling behavior with consistent daily patterns, though operational characteristics vary with solar irradiance conditions, emphasizing the need for proper sizing or auxiliary backup integration.

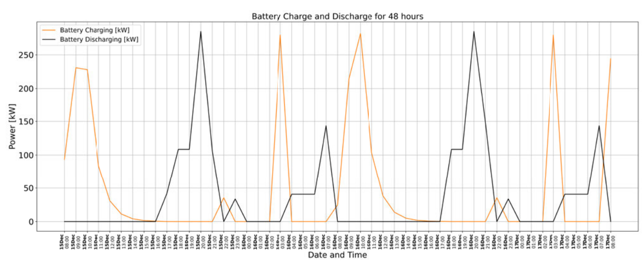

FIGURE 14. Temporal evolution of battery charging and discharging during a 48 hours period in December.

Figure 15 further confirms these trends: the state of charge remains generally high during midday hours (10:00 to 20:00) throughout most of the year but drops significantly during winter months (December-January) due to reduced solar generation while demand remains steady.

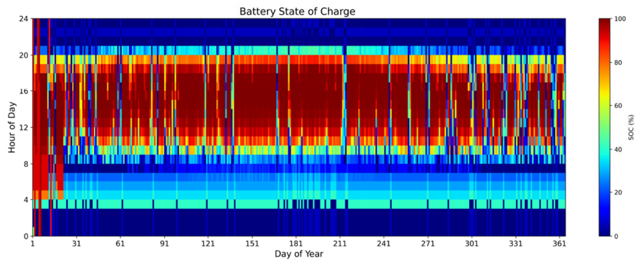

FIGURE 15. Annual DMAP of the battery state of charge.

The quantitative performance of the storage system, derived from the HOMER simulation results, is summarized in Table 14. These indicators confirm the efficient role of the battery in stabilizing the DC bus and enhancing renewable utilization.

TABLE 14. Annual performance, energy balance and economic parameters of the storage system.

Parameter	Symbol	Value	Unit
Number of batteries	N_{bat}	106	units
Total battery capacity	C_{nom}	661	kWh
Usable capacity	C_{usable}	661	kWh
Energy charged	$E_{batt,in}$	337,372	kWh/year
Energy discharged	$E_{batt,out}$	321,112	kWh/year
Storage losses	$E_{batt,loss}$	16884	kWh/year
Storage Depletion E_{SD}	624	kWh/year	
Annual throughput	$E_{batt,ann}$	329,454	kWh/year
Autonomy duration	t_{aut}	4.88	hours
Storage wear cost	C_{wear}	0.0054	€/kWh
Lifetime energy throughput	E_{life}	3,294,537	kWh
Battery capital cost	$C_{cap,bat}$	300	€
Battery replacement cost	$C_{rep,bat}$	200	€
Battery O&M cost	$C_{O\&M,bat}$	10	€/year

The energy flows indicate that $E_{batt,out}$ represents approximately 95.1% of $E_{batt,in}$, implying a round trip efficiency close to 95%. The resulting storage losses amount to 16,884 kWh/year, reflecting the inherent inefficiencies of the charge–discharge process in lithium based battery systems. This performance confirms the effective integration of the storage subsystem within the overall energy management strategy. Consequently, the battery contributes to load smoothing and peak shaving, thereby enhancing system autonomy and operational stability.

3) CONVERTER

The bidirectional converter ensures power flow management between the DC and AC buses, operating either as an inverter (DC/AC) or rectifier (AC/DC) depending on energy balance conditions. Figures 16–18 illustrate its dynamic behavior during December.

During the period of December 15-17, the inverter (green curve) exhibits regular daily operation, starting in the morning hours (around 07:00-08:00), reaching peak values of approximately 300-330 kW, and maintaining operation until the late afternoon (17:00-18:00).

This behavior closely follows the photovoltaic generation profile, indicating that the inverter primarily transfers surplus DC power from the PV array to the AC side during periods of sufficient solar production (E_{inv}).

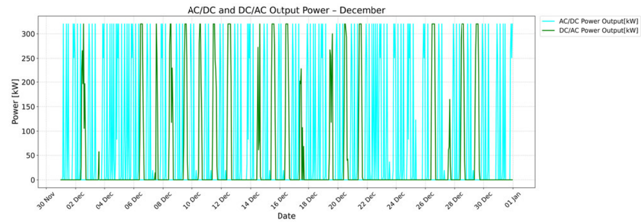

FIGURE 16. Converter output power in both operating modes during December.

Conversely, the rectifier (cyan curve) operates intermittently throughout the period, with shortnduration peaks occurring mainly during nighttime and early morning hours.

The rectifier power also reaches values up to approximately 300-330 kW, corresponding to situations of reduced PV generation or low battery state of charge, during which the system imports energy from the grid to support battery charging or supply the DC load (E_{rect}).

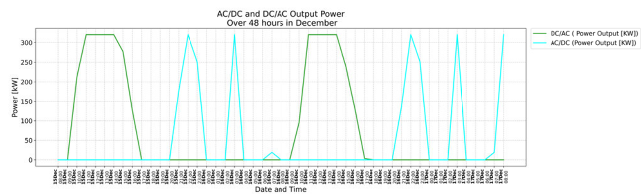

FIGURE 17. Converter output power over a 48-hours period in December.

Figure 18 confirms these seasonal trends: inverter operation dominates during daytime hours (06:00–18:00), while rectifier activity is sporadic and limited to winter or low solar conditions. This complementary operation ensures optimal bidirectional power management between renewable generation, storage, and the grid interface.

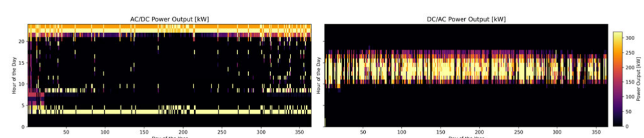

FIGURE 18. Annual DMAP of inverter and rectifier operation.

The main technical and operational parameters of the converter subsystem are summarized in Table 15. The system incorporates a bidirectional converter rated at 320 kW, operating for 2,229 h/year in inverter mode and 2,041 h/year in rectifier mode.

The overall conversion efficiency is 95%, ensuring minimal power losses between the DC and AC subsystems.

TABLE 15. Annual performance and economic parameters of the bidirectional converter (Eaton Power Xpert 1000 kW).

Parameter	Symbol	Value
Rated power	P_{rated}	323 kW
Efficiency	η_{conv}	98%
Inverter operation time	t_{inv}	2,236 h/yr
Rectifier operation time	t_{rect}	2044 h/yr
Average inverter power	$P_{\text{inv,avg}}$	55.2 kW
Average rectifier power	$P_{\text{rect,avg}}$	51.7 kW
Inverter energy	E_{inv}	485,996 kWh/yr
Rectifier energy	E_{rect}	452,613 kWh/yr
Conversion losses	E_{loss}	9,237 kWh/yr
Converter capital cost	$C_{\text{cap,conv}}$	350 €/kW
Converter replacement cost	$C_{\text{rep,conv}}$	300 €/kW
Converter O&M cost	$C_{\text{O\&M,conv}}$	120 €/year

The inverter thus handles the majority of annual energy transfer, efficiently routing photovoltaic power to the grid or DC bus, while the rectifier provides limited but crucial support during low generation periods. This configuration contributes to overall system stability, optimizing renewable utilization and minimizing grid dependency.

4) ELECTRICAL GRID

Figure 19 illustrates the annual hourly exchanges between the hybrid system and the grid. Grid sales occur mainly between 09:00 and 16:00, with peak injections reaching about 300–350 kW, reflecting significant daytime solar production. Grid purchases, by contrast, occur mostly during nighttime and early morning hours, are intermittent, and generally remain limited, indicating reduced dependence on the grid outside solar generation periods.

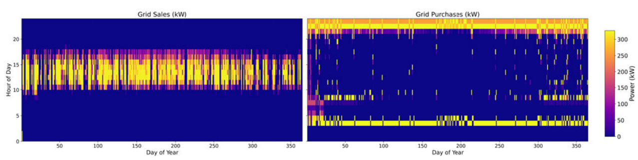

FIGURE 19. DMAP of power injected into and withdrawn from the electrical grid.

Figure 20, detailing a 48 hours period, confirms this trend: significant daytime exports reach about 300–330 kW, corresponding to peak solar production hours. Grid imports remain limited and intermittent, appearing mainly as short evening (around 22:00) or nighttime (02:00–04:00) peaks. Overall, the system demonstrates strong energy autonomy, with grid reliance restricted to brief periods when solar generation and storage are insufficient.

C. ANALYSIS OF THE OVERALL ENERGY OPERATION OF THE HYBRID SYSTEM

Figures 21 and 22 illustrate the energy management strategy and the cyclic operation of the hybrid system over a representative three-day period in December, with a detailed focus on a single day.

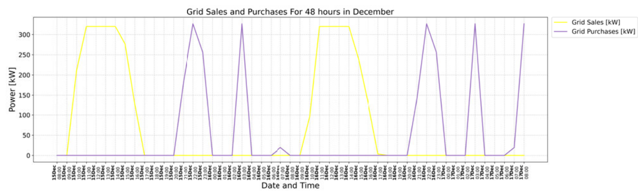

FIGURE 20. Power purchased from and sold to the grid over a 48 hours period in December.

TABLE 16. Annual emissions of major pollutants.

Pollutant	Quantity	Unit
Carbon dioxide (CO_2)	291,889	kg/year
Carbon monoxide (CO)	0	kg/year
Unburned hydrocarbons	0	kg/year
Particulate matter (PM)	0	kg/year
Sulfur dioxide (SO_2)	1265	kg/year
Nitrogen oxides (NO_x)	619	kg/year

TABLE 17. Global economic indicators.

Indicator	Value	Unit
NPC	2,376,450.00	€
COE	0.1098	€/kWh
Operating Costs	133,258.10	€

Phase 1 (nighttime): In the absence of solar generation (blue curve), the EV charging demand (red curve) is mainly supplied by the grid via the AC/DC converter (purple curve and light-blue curve), with noticeable peaks occurring around 03:00 and after 22:00. During the late night and early morning hours, the battery (black curve) also contributes by discharging to partially supply the DC load. In this phase, the converter ensures AC to DC power conversion, allowing the EV charging demand to be met while maintaining system continuity in the absence of PV production.

In Phase 2, or the morning transition (around 07:00–08:00), PV generation starts increasing progressively and reaches significant levels during the morning. The generated solar power is first used to supply the DC load and to recharge the battery (orange curve). As PV production continues to rise, the DC/AC converter (green curve) becomes active, enabling surplus energy to be injected into the grid (yellow curve). During this phase, the reliance on the grid is progressively eliminated.

Phase 3, during the daytime period, PV generation reaches its maximum values (around 650–700 kW), fully covering the EV charging demand and ensuring effective battery charging. The excess solar energy is exported to the grid, resulting in sustained grid sales. In this phase, the converter operates predominantly in inverter mode, reflecting optimal operating conditions and high system energy autonomy. In the late afternoon, PV output gradually decreases, leading to the end of battery charging. The battery then shifts to discharge mode to maintain the supply of DC loads. This allows the system to continue operating autonomously despite the reduction in solar generation, while the converter maintains power balance within the system.

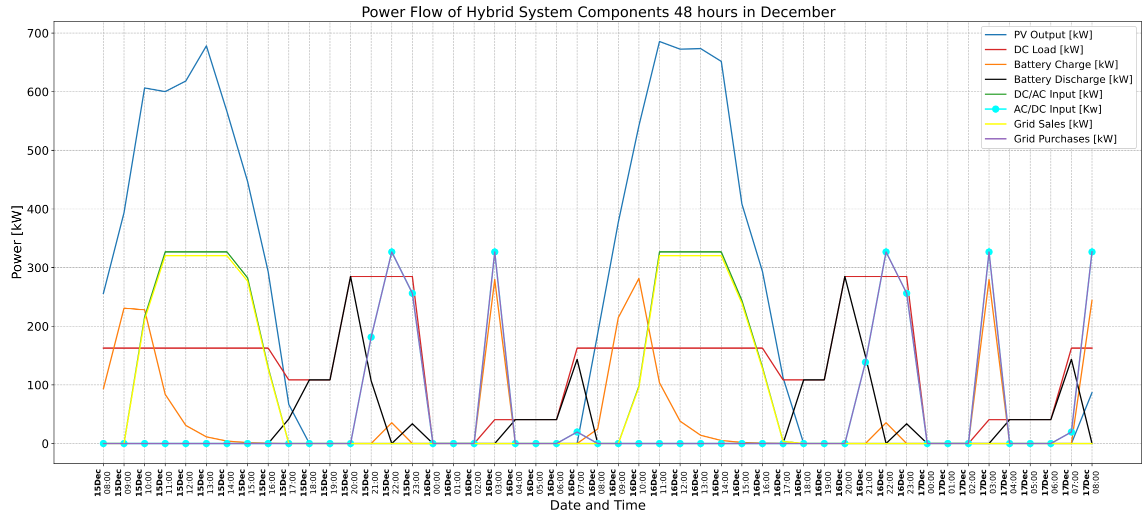

FIGURE 21. Power variation of the sources over 48 hours in December.

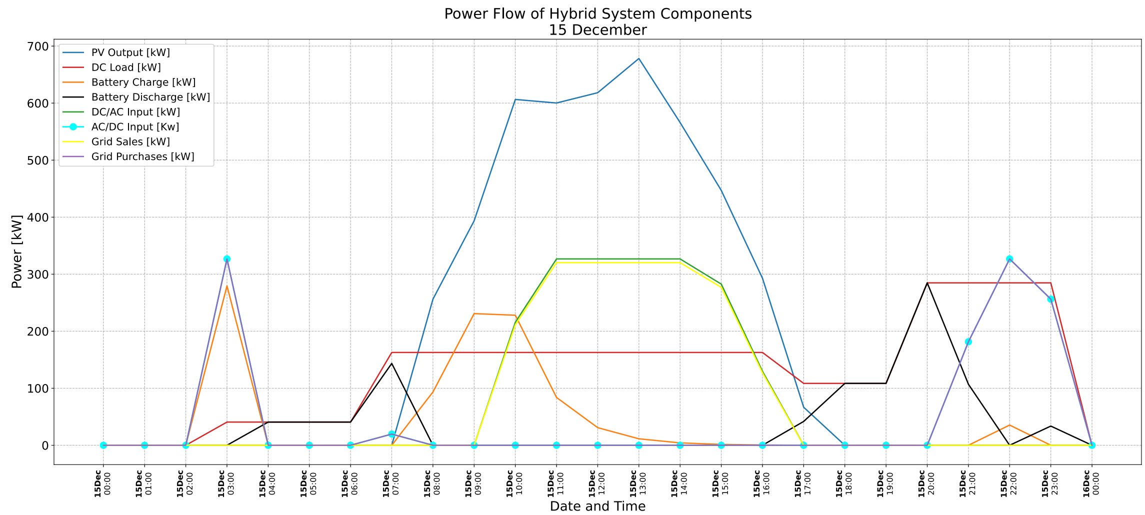

FIGURE 22. Zoomed in view of the power variation of hybrid system sources on a representative day.

In Phase 4, corresponding to the evening period (between 18:00 and 22:00), the battery becomes the main energy source, discharging to meet the EV charging demand. During this period, grid contribution remains negligible or absent, highlighting the system's ability to operate autonomously based on stored energy.

Finally, Phase 5, corresponding to the late evening (22:00 to midnight), battery discharge reaches its operational limits, which triggers grid intervention. This is evidenced by the activation of grid purchases (purple curve) and the corresponding AC/DC converter operation (light-blue curve). Grid power is used to sustain the EV charging station and may also contribute to partial battery recharging, potentially taking advantage of off-peak electricity tariffs.

Overall, this operating scheme highlights a well coordinated hybrid energy system in which solar generation ensures daytime supply, the battery provides continuity during transition periods, and the grid acts solely as a backup source. This strategy guarantees reliable operation of the EV charging station, minimizes grid dependency, and maximizes local energy self consumption.

D. ENVIRONMENTAL IMPACT ANALYSIS

Based on a combination of photovoltaic panels, batteries, and a bidirectional converter with grid support, the system ensures a reliable power supply while limiting pollutant emissions. Although reliance on the electrical grid still generates CO_2 (291,868 kg/year), SO_2 (1,265 kg/year), and NO_x (619 kg/year), other pollutants such as carbon monoxide, unburned hydrocarbons, and particulate matter are completely absent. These results confirm a significant reduction in the carbon footprint of electric mobility [40].

TABLE 18. Comparison of optimal system configurations.

Scenario	COE (€/kWh)	NPC (€)	Op. Cost (€/yr)	Init. Cost (€)	PV Cost (€)	Aut. (h)	Batt. (units)	Ren. Frac (%)	Emissions (kg/yr)		
									CO_2	SO_2	NO_x
PV+Battery+Grid *(optimal)*	0.110	2,376,450	133,258	653,753	509,000	4.88	106	72.4	291,889	1,265	619
PV+Grid	0.109	2,563,729	150,433	619,009	509,000	—	—	65.3	398,753	1,729	845
Battery+Grid	0.230	3,528,349	266,041	89,104	—	5.20	113	0	772,876	3,351	1,639
Grid	0.245	3,764,030	282,655	110,009	—	—	—	0	766,062	3,321	1,624

TABLE 19. Sensitivity analysis of key techno-economic parameters.

Inv. Eff. (%)	PV Der. (%)	COE (€/kWh)	NPC (€)	Op. Cost (€/yr)	Ren. Frac (%)
95	75	0.1283	2,559,897	147,667	69.21
95	88	0.1112	2,379,267	131,800	74.60
98	75	0.1274	2,562,942	147,858	69.11
98	**88**	**0.1098**	**2,376,450**	**133,258**	**72.41**

E. ECONOMIC EVALUATION OF THE SYSTEM

Economic analysis is essential to assess the viability of hybrid RE systems, which are often perceived as costly compared to conventional solutions. A comprehensive financial assessment, based on key indicators, allows evaluating whether the proposed system can sustainably meet energy needs at an acceptable cost.

Table 17 presents three major economic indicators: the NPC, the COE, and the operating costs. The NPC encompasses initial investments, replacements, operating costs, and discounted cash flows, reflecting a significant investment to guarantee reliable energy autonomy. Beyond environmental benefits, the amount indicated in the table is highly advantageous compared to the investment required for establishing a conventional hydrocarbon distribution station. The COE remains competitive compared to the grid electricity price, confirming the system's economic viability. Operating costs, on the other hand, represent only 1% of the total amount, reflecting regular expenses for system maintenance and operation [41].

In addition, the cost breakdown per component summarizes the overall project. The initial investment, or capital cost, amounts to 653,752.84 €, with an additional 131,932.23 € allocated for equipment replacement over time. Operating and maintenance costs are estimated at 1,614,609.88 €, covering system upkeep and operational management. No fuel is used (0.00 €), which is consistent with a system relying exclusively on renewable sources without thermal generators.A decommissioning or recycling cost of -23,845.33 € is considered as the residual value at the end of the project lifetime. Consequently, the system's net cost reaches 2,376,450.0 €, fully consistent with the NPC previously indicated.

These results demonstrate that, despite a high initial investment, the proposed hybrid system is highly profitable and economically viable in the long term, thanks to low cost energy production and significant operational revenues.

In summary, the hybrid energy system developed in this study intelligently integrates renewable sources, battery storage, and grid interaction to effectively meet targeted demand, particularly for EV charging. Simulations validated its capacity to meet energy requirements while ensuring a continuous and reliable power supply. From an environmental perspective, the integration of renewable energies contributes to reducing pollutant emissions and supports a more sustainable approach. Finally, the technoeconomic assessment confirmed the coherence and feasibility of the project, showing that it represents a technically efficient, balanced, and well suited solution for the current requirements of sustainable energy supply.

This analysis highlights the efficiency of intelligent and optimized energy management, primarily based on solar self consumption and the rational use of battery storage. The occasional and limited use of the grid demonstrates the performance and appropriate sizing of the hybrid system. This operational strategy also contributes to cost control by limiting energy exchanges with the grid. Moreover, this study provides a reversible vision of the system: it demonstrates its ability to operate autonomously under favorable conditions while maintaining the possibility of relying on the grid in case of exceptional needs or climatic constraints. This flexibility paves the way for a gradual transition toward a 100% renewable system, notably through increased storage capacity, ensuring full coverage of demand even in the absence of solar production.

F. SENSITIVITY ANALYSIS AND COMPARISON OF ALTERNATIVE CONFIGURATIONS

To validate the robustness of the optimal configuration and assess the added value of each system component, two complementary analyses were conducted under identical simulation conditions using HOMER Pro.

To further strengthen the robustness of the proposed sizing methodology and to account for different possible system configurations, a comparative analysis of four alternative scenarios was conducted. The scenarios differ in their component combinations while sharing the same meteorological dataset, EV demand profile, and optimization framework, ensuring a fair and consistent basis for comparison. Table 18 summarizes the key technical, economic, and environmental performance indicators for each scenario.

These results highlight the importance of combining photovoltaic generation with battery storage to ensure a balanced system. The proposed PV–battery–grid configuration offers a more efficient and sustainable solution, improving energy autonomy while reducing reliance on the grid compared to the alternative scenarios.

A sensitivity analysis was performed to evaluate the influence of component performance uncertainties on the optimal system design. Two parameters were varied: the converter efficiency ($\eta_{\text{conv}} = 95\%$ and 98%) and the PV derating factor ($f_d = 75\%$ and 88%). Table 19 summarizes the results of the four sensitivity scenarios.

The base optimal configuration (Scenarios: $\eta_{\text{conv}} = 98\%$, $f_d = 88\%$) corresponds to the initial HOMER simulation result. Across all sensitivity scenarios, the COE varies by less than 3% (0.1098–0.1283 €/kWh), the NPC remains within 2.37–2.56 M€, and the renewable fraction between 72% and 74%, confirming the robustness of the proposed hybrid system to realistic component performance uncertainties.

V. CONCLUSION

This paper presented the design and sizing of a hybrid energy production system combining PV power, battery storage, and the electrical grid to supply an EV charging station. The study was conducted in the village of Mesra, located in the Mostaganem province in western Algeria. The approach aimed to determine the appropriate, efficient, and optimal configuration of the station, reflecting the interactions and complementarities among the different components of the system. To achieve this, an analysis was performed to model the daily charging profile of the station. The study considered three representative EV models (Dacia Spring, Tesla Model 3, and Renault Zoe) and an infrastructure of five charging stations. The resulting model simulated the temporal distribution of residential loads across four different periods. This approach allowed determining the optimal size of the hybrid systems and improving their integration according to real consumption patterns.

The technical analysis demonstrated that photovoltaic generation covers a large share of the station's energy demand, particularly during daytime, thanks to a well dimensioned solar array. The battery ensures supply continuity during periods without solar irradiation, while the grid provides occasional backup to secure the power supply. Simulation curves confirmed that the designed system is well optimized and energetically synchronized. Although the system involves multiple operational phases across its components, it is worth noting that for half of the day the load is supplied by PV, one quarter by the battery, and one quarter by the grid. This distribution highlights the improvement such a structure provides to the central grid.

Beyond technical aspects, the environmental analysis revealed remarkable ecological performance, with the complete elimination of critical pollutants such as CO, unburned hydrocarbons, and particulate matter. Although limited reliance on the electrical grid still results in residual emissions (291,889 kg CO_2/year, 1,265 kg SO_2/year, and 619 kg NO_x/year), this configuration confirms a significant reduction in the overall carbon footprint compared to conventional solutions, thereby demonstrating the environmental relevance and sustainability of such infrastructures.

From an economic perspective, the evaluation of the hybrid system demonstrates attractive financial performance, with a COE of 0.1098 €/kWh and operating expenses limited to 133,285.1 €, representing approximately 1% of the total system cost. Despite a relatively high initial capital investment of 653,752.84 €and a NPC of 2,376,450 €, the proposed hybrid architecture remains economically viable by ensuring reliable long term energy supply and reducing exposure to fossil fuel price volatility, thus reinforcing the financial attractiveness of renewable powered EV charging infrastructures.

Moreover, the results obtained from the energy based indicators confirm the robustness of the proposed configuration. The system achieved a SS rate of 74.2%, indicating that a large share of the station's annual energy demand is covered by photovoltaic generation and battery storage, while the grid provides complementary support during periods of low renewable availability. In parallel, the SC index reached 59%, showing that more than half of the total PV generation was directly consumed locally or stored in the battery. Although a portion of the energy is exported to the grid, this level of self consumption reflects an efficient local energy utilization strategy, contributing to improved system autonomy and reduced grid dependency. The sensitivity analysis further reinforces these findings, as the comparison across multiple scenarios consistently confirms the robustness and optimality of the proposed configuration under varying techno-economic conditions. These metrics confirm the technical maturity of the system and its ability to operate effectively under realistic operating conditions.

This work provides a modest contribution to the Algerian energy mix program, which has witnessed significant progress in recent years, aiming to reduce greenhouse gas emissions and mitigate energy disruptions, while moving toward a more sustainable environment. For more complex and dynamic energy systems, a promising perspective would be the integration of intelligent energy management mechanisms based on artificial intelligence (AI).

REFERENCES

[1] International Energy Agency. (Oct. 2024). *Renewables 2024: Analysis and Forecast to 2030*. [Online]. Available: https://www.iea.org/reports/renewables-2024

[2] Y. Kebbati and L. Baghli, "Design, modeling and control of a hybrid grid-connected photovoltaic-wind system for the region of adrar, Algeria," *Int. J. Environ. Sci. Technol.*, vol. 20, no. 6, pp. 6531–6558, Jun. 2023.

[3] M. Boubekeur and A. Argilos, "Integration of renewable energy sources in Algeria: Achievement and perspective," *J. Modern Economy Sustain. Develop.*, vol. 6, no. 1, pp. 71–83, Jun. 2023. [Online]. Available: https://asjp.cerist.dz/en/article/225924

[4] M. Werner, P. Porwisiak, M. Kryza, L. Gawuc, K. Szymankiewicz, M. Holland, A. Drzeniecka-Osiadacz, K. Skotak, and M. Vieno, "Environmental, health and economic benefits of emission reduction in residential sector—A case study for Poland," *Atmos. Pollut. Res.*, vol. 16, no. 1, Jan. 2025, Art. no. 102360.

[5] S. Hardman, K. L. Fleming, E. Khare, and M. M. Ramadan, "A perspective on equity in the transition to electric vehicle," *MIT Sci. Policy Rev.*, vol. 2, pp. 46–54, May 2021.

[6] A. Bouraiou, A. Necaibia, N. Boutasseta, S. Mekhilef, R. Dabou, A. Ziane, N. Sahouane, I. Attoui, M. Mostefaoui, and O. Touaba, "Status of renewable energy potential and utilization in Algeria," *J. Cleaner Prod.*, vol. 246, Feb. 2020, Art. no. 119011. [Online]. Available: https://www.sciencedirect.com/science/article/pii/S0959652619338818

[7] A. Meslem and M. Baroudi, "Factors influencing the adoption of electric vehicles in Algeria: A review and conceptual framework," *Algerian Sci. J. Platform (ASJP)*, vol. 8, no. 1, pp. 310–333, May 2025. [Online]. Available: https://asjp.cerist.dz/en/article/267024

[8] C. Li, Y. Shan, L. Zhang, L. Zhang, and R. Fu, "Techno-economic evaluation of electric vehicle charging stations based on hybrid renewable energy in China," *Energy Strategy Rev.*, vol. 41, May 2022, Art. no. 100850.

[9] A. Haffaf, F. Lakdja, and D. Ould Abdeslam, "Experimental performance analysis of an installed microgrid-based PV/battery/EV grid-connected system," *Clean Energy*, vol. 6, no. 4, pp. 599–618, Aug. 2022.

[10] B. Robisson, V.-L. Ngo, L. Marchadier, M.-F. Bouaziz, and A. Mignonac, "PV sizing for EV workplace charging stations—An empirical study in france," *Appl. Sci.*, vol. 13, no. 18, p. 10128, Sep. 2023.

[11] R. Lamedica, A. Ruvio, P. Falessi, M. Maccioni, E. Sammartino, and M. Palumbo, "Power unit architecture in a high-power charging system for EVs," *Int. J. Electr. Power Energy Syst.*, vol. 149, Jul. 2023, Art. no. 109052.

[12] V. J. Prakash, M. R. Paul, S. Kannan, A. Rufus, and A. Bhuvanesh, "Green power ev charging station design and analysis for electric vehicles," *Int. J. Electr. Electron. Res.*, vol. 12, no. 2, pp. 345–351, Apr. 2024.

[13] A. Abodwair, M. Guneser, M. Khaleel, Y. Nassar, H. El-Khozondar, and A. Elbaz, "Feasibility assessment of hybrid renewable energy based EV charging station in libya," *Sol. Energy Sustain. Develop. J.*, vol. 13, no. 2, pp. 311–349, Nov. 2024.

[14] E. Karapidakis, M. Nikologiannis, M. Markaki, G. Kouzoukas, and S. Yfanti, "Enhancing renewable energy integration and implementing EV charging stations for sustainable electricity in crete's supermarket chain," *Energies*, vol. 18, no. 3, p. 754, Feb. 2025.

[15] SolarGIS. (2024). *Solar Resource Maps of Algeria*. [Online]. Available: https://solargis.com/maps-and-gis-data/download/algeria

[16] NASA Langley Research Center, Hampton, VI, USA. (2024). *Nasa Power: Prediction of Worldwide Energy Resources*. [Online]. Available: https://power.larc.nasa.gov/

[17] A. K. Tripathi, G. S. Lakshmi, H. Mishra, S. Chapala, M. Alwetaishi, F. Atamurotov, N. E. Benti, S. Sura, and C. A. Saleel, "Integration of solar PV panels in electric vehicle charging infrastructure: Benefits, challenges, and environmental implications," *Energy Sci. Eng.*, vol. 13, no. 4, pp. 2135–2152, Feb. 2025.

[18] G. Cheikh, C.-G. Haba, and H. A. Bentounes, "Study of a hybrid system (PV-battery-Grid) for electric vehicle charging stations," in *Proc. IEEE Int. Conf. Expo. Electr. Power Eng. (EPEi)*, Oct. 2024, pp. 368–373.

[19] E. Y. Pramono, A. Rommyonegge, B. A. Soedjarno, K. M. Banjar-Nahor, and N. Hariyanto, "Optimization of renewable energy allocation to reduce network vulnerability risk under intentional transmission attacks," *IEEE Access*, vol. 12, pp. 26492–26505, 2024.

[20] K. Vidhya and K. Krishnamoorthi, "A hybrid technique for optimal power quality enhancement in grid-connected photovoltaic interleaved inverter," *Energy Environ.*, vol. 35, no. 1, pp. 244–274, Feb. 2024.

[21] World Bank Group. (2019). *Global Solar Atlas*. [Online]. Available: https://globalsolaratlas.info/

[22] R. Grab, F. Hans, M. I. R. Flores, H. Schmidt, S. Rogalla, and B. Engel, "Modeling of photovoltaic inverter losses for reactive power provision," *IEEE Access*, vol. 10, pp. 108506–108516, 2022.

[23] Union Technique de l'Electricite (UTE), "Installations electriques a basse tension—Guide pratique—Installations photovoltaïques sans stockage et raccordees au reseau public de distribution [low-voltage electrical installations—Practical guide—Photovoltaic installations without storage connected to the public distribution network," AFNOR, Paris, France, Tech. Rep. C 15-712-1, 2013. [Online]. Available: https://www.photovoltaique.guidenr.fr/informations_techniques/conception-photovoltaique-raccordee-reseau/chute-tension.php

[24] T. Khatib, A. Mohamed, and K. Sopian, "A review of photovoltaic systems size optimization techniques," *Renew. Sustain. Energy Rev.*, vol. 22, pp. 454–465, Jun. 2013.

[25] Trina Solar Limited. (2019). *TSM-PE15h 340-355w Multicrystalline Module Datasheet*. [Online]. Available: https://fr.enfsolar.com/pv/panel-datasheet/crystalline/48871

[26] C. Deline, B. Sekulic, J. Stein, S. Barkaszi, J. Yang, and S. Kahn, "A performance and economic analysis of distributed power electronics in photovoltaic systems," *Nature Energy*, vol. 2, no. 6, p. 17032, 2017.

[27] Eaton Corporation. (2020). *Power Xpert 9395p 1000 KVA UPS Technical Specifications*. [Online]. Available: https://www.eaton.com/us/en-us/catalog/backup-power-ups-surge-it-power-distribution/power-xpert-9395p-high-performance-ups.html

[28] U.-M. Choi, "Study on effect of installation location on lifetime of PV inverter and DC-to-AC ratio," *IEEE Access*, vol. 8, pp. 86003–86011, 2020.

[29] M. M. Hosen, M. S. Alam, S. Rashid, and S. M. G. Mostafa, "Optimized economic dispatch and battery sizing in wind microgrids: A depth of discharge perspective," *Electricity*, vol. 6, no. 3, p. 51, Sep. 2025. [Online]. Available: https://www.mdpi.com/2673-4826/6/3/51

[30] Discover Battery. (2023). *Aes 42-48-6650 Technical Specifications*. [Online]. Available: https://discoverbattery.com/products/aes-battery-series

[31] M. Benali, C. Ghenai, and I. Janajreh, "Measures to promote renewable energy for electricity generation in Algeria," *Sustainability*, vol. 12, no. 4, p. 1468, Feb. 2020. [Online]. Available: https://www.mdpi.com/2071-1050/12/4/1468

[32] A. F. Z. Bochra, "Optimisation du dimensionnement et de la gestion dèun systéme multi-sources avec stockage hybride, application: Sud algérien," Ph.D. thesis, Dept. Elect. Eng., Abdelhamid Ibn Badis-Mostaganem, 2025.

[33] M. Guezgouz, J. Jurasz, B. Bekkouche, T. Ma, M. S. Javed, and A. Kies, "Optimal hybrid pumped hydro-battery storage scheme for off-grid renewable energy systems," *Energy Convers. Manage.*, vol. 199, Nov. 2019, Art. no. 112046.

[34] M. A. Islam, M. M. N. Ali, A. Al Mamun, M. S. Hossain, M. H. Maruf, and A. S. M. Shihavuddin, "Optimizing energy solutions: A techno-economic analysis of solar-wind hybrid power generation in the coastal regions of Bangladesh," *Energy Convers. Manag., X*, vol. 22, Apr. 2024, Art. no. 100605. [Online]. Available: https://www.sciencedirect.com/science/article/pii/S2590174524000837

[35] F. Z. B. Amrani, S. Marih, I. Missoum, F. Boutlilis, and B. Bekkouche, "Site suitability analysis of wind energy resources in different regions of Algeria's southwestern highland," *Int. J. Renewable Energy Develop.*, vol. 13, no. 1, 2024. [Online]. Available: https://ijred.cbiore.id/index.php/ijred/article/view/56476

[36] A. M. B. Francisco, J. Monteiro, and P. J. S. Cardoso, "A digital twin of charging stations for fleets of electric vehicles," *IEEE Access*, vol. 11, pp. 125664–125683, 2023.

[37] HOMER Energy by UL and National Renewable Energy Laboratory (NREL). *OMER: Hybrid Optimization of Multiple Energy Resources*. Accessed: 2024. [Online]. Available: https://www.homerenergy.com

[38] HOMER Energy. (2024). *Converter—Homer Pro Documentation*. Accessed: 2024. [Online]. Available: https://homerenergy.com/products/pro/docs/latest/converter.html

[39] (2024). *PV Derating Factor—Homer Pro Documentation*. Accessed: 2024. [Online]. Available: https://homerenergy.com/products/pro/docs/latest/pv_derating_factor.html

[40] A. U. Rehman, H. M. Khalid, and S. M. Muyeen, "Grid-integrated solutions for sustainable EV charging: A comparative study of renewable energy and battery storage systems," *Frontiers Energy Res.*, vol. 12, Sep. 2024, Art. no. 1403883.

[41] Y. Ayed, R. Al Afif, P. Fortes, and C. Pfeifer, "Optimal design and techno-economic analysis of hybrid renewable energy systems: A case study of Thala city, Tunisia," *Energy Sour., B, Econ., Planning, Policy*, vol. 19, no. 1, Dec. 2024, Art. no. 2308843.

GHIZLENE CHEIKH received the joint B.Eng. and M.Sc. degree in electrotechnical engineering in energy and environment from the Higher School of Applied Sciences, Tlemcen, Algeria, in 2020. She is currently pursuing the Ph.D. degree with the ERSE Laboratory and the LSS Laboratory, Abdelhamid Ibn Badis University of Mostaganem, Algeria. She is a member of the PRFU Project and has completed several projects, presenting her work at conferences, such as the IEEE International Conference on Artificial Intelligence and Green Energy and the IEEE International Conference on Electrical and Power Engineering. Her research interests include renewable energy, energy management, and the integration of artificial intelligence in renewable energy for forecasting and operational management.

FATIMA BOUTLILIS received the State Engineering degree in electrotechnical engineering from the University of Science and Technology of Oran-Mohamed Boudiaf (USTO MB), Algeria, in 1988, and the Ph.D. degree in renewable energy sciences, in 2015. She is currently a Teacher-Researcher with the Department of Electrical Engineering, Abdelhamid Ibn Badis University of Mostaganem, Algeria. Her research interests include the design and dimensioning of photovoltaic generators, the integration of artificial intelligence for energy forecasting and management, and the development of smart renewable energy systems. She has extensive experience in modeling, simulation, and intelligent control of energy systems.

JÂNIO MONTEIRO received the Ph.D. degree in electrical and computer engineering from the Instituto Superior Técnico, University of Lisbon, Portugal. He is currently a Professor with the Institute of Engineering, Universidade do Algarve, Faro, Portugal. He is a member of the Coordination Commission of the Research Center in Cyber Physical Systems; the President of the Board of Directors of CINTAL, a technological research center, Algarve; and the President of the Technical-Scientific Council, Institute of Engineering, University of Algarve. He has participated in 14 European research and development projects funded by European Union, five as Principal Investigator (PI), and eight national projects with local companies, acting as PI in two. He has edited three books and published more than 80 scientific works. His research interests include smart grids, sensor networks, the Internet of Things, communication networks, and neural computing.

CRISTIAN-GYŐZŐ HABA (Member, IEEE) received the B.Sc. degree in electrical engineering and the Ph.D. degree in automatic control from the Gheorghe Asachi Technical University of Iaşi, Romania, in 1988 and 2000, respectively, with a focus on the development of digital design techniques. He is currently a Professor with the Faculty of Electrical Engineering, Gheorghe Asachi Technical University of Iaşi. He is also the Director of the Department of Electrical Engineering. He is a member of the Commission for Resource Management and Institutional Development of the University Senate and the Research Team at the Energy Conversion and Motion Control Systems Research Centre (SCECM). His research interests include the design of digital systems, microcontroller-based systems, online education (remote and virtual laboratories), and web-based measurement systems applied to light and environment monitoring, as well as design and monitoring of solar panels using machine learning techniques. He is a member of ACM and EAI. Since 2019, he has been the Chair of the IEEE Romania Education Chapter.

HADJ ADDA BENTOUNES received the B.Sc. degree in electrical engineering from the Higher School of Electricity, Gif-sur-Yvette, France, in 1980, and the Ph.D. degree in gas and plasma physics from the University of Orsay, France, in 1984. Since 1985, he has been a Faculty Member with the Abdelhamid Ibn Badis University of Mostaganem, Algeria, and has been a Professor, since 2014. He founded the Department of Metrology for Mostaganem region and authored a monograph on territorial planning and sustainable development. He is a member of the ERSE Laboratory. He has supervised several doctoral and graduate theses in areas, including materials science, environmental monitoring, and hybrid energy systems. He has managed multiple PRFU-funded research projects. He has published extensively in international journals and conferences, contributing to topics such as desertification monitoring, photovoltaic energy forecasting, and the structural and electronic properties of advanced materials. His current research interests include environmental modeling, renewable energy systems, and the integration of artificial intelligence for forecasting and energy management.